Theoretical and Applied Climatology (2024) 155:371–397
https://doi.org/10.1007/s00704-023-04640-9

RESEARCH

Utilizing advanced and modified conventional trend methods to evaluate multi-temporal variations in rainfall characteristics over India

Ashish Dogra[1] · Chhabeel Kumar[1] · Ankit Tandon[1]

Received: 19 June 2023 / Accepted: 2 September 2023 / Published online: 16 September 2023

Abstract
Adequate and consistent rainfall is essential for sustaining water resources, agricultural production, and overall economy of a nation. To explore the variability and changes in rainfall system, the most common and widely employed conventional trend methods are linear regression (LR) and Mann-Kendall (MK) trend tests. These methods are often subject to inconsistent results with respect to the extent of changes reported in rainfall patterns. This study utilizes the advanced LR i.e., quantile regression (QR) and the modified MK (m-MK) trend methods to investigate the retrospective rainfall characteristics and associated trends for multi-temporal periods i.e., long-term (1951–2020), bifurcated (pre-1985 and post-1985), and most-recent (2000–2020), over different climate zones of India. Furthermore, temporal evolution and trend consistency (stability) were examined by comparing multi-temporal slope coefficients at various quantiles (τ) of rainfall distribution. The long-term trends in general rainfall characteristics (GRCs) exhibited drying patterns, while opposite increasing trends were observed in extreme rainfall characteristics (ERCs) for most of the study region. The results of QR at median tail ($\tau = 0.5$) were more or less consistent with the results of m-MK test. Interestingly, an increase in the trend significance and magnitude was observed at higher quantiles ($\tau > 0.8$). The bifurcated and long-term periods showed contrasting results in rainfall characteristics, suggesting trend instability whereas during pre-1985, post-1985, and most-recent periods, the temporal evolution of GRCs revealed a systematic increment in positive trend significance. Altogether, the advanced and modified trend assessment in the present research compliments conventional trend methods with improved trend detection and trend consistency identification.

1 Introduction

Climate change is by far the most relevant and ever-evolving topics of concern for the scientific community. The consequences of climate change include global warming, melting of glaciers, rising sea surface temperature and sea level, and rapidly increasing extreme weather events (Koutsoyiannis 2020). These imposed implications of climate change are likely to be more eminent in systems that are vulnerable to temperature change. For instance, in hydrological system, for each °C rise in temperature, atmosphere can hold 6–7% of more water vapor, which might result in 2–3% rise in global precipitation (Allen and Ingram 2002; Marvel et al. 2019). However, the transformation of atmospheric moisture into rainfall is not uniform, which is majorly due to the limits imposed by changes in moist-adiabatic temperature lapse rate and associated moisture availability (O'Gorman and Schneider 2009). Consequently, the transposed frequency and intensity of rainfall events over a large spatial domain become highly uncertain and heterogeneous (Chou and Lan 2012; Feng and Fu 2013; Marvel et al. 2017). Therefore, it is expected that the continued global warming will intensify the global water cycle, leading to changes in global monsoon precipitation, including the regional precipitation patterns and very wet and very dry weather and climate events, particularly over Asia (high confidence) at 1.5 °C global warming (IPCC, 2023). The anticipated alterations in precipitation patterns in particular, which is a pivotal climate factor of a region, will directly impact the stream flow pattern, ground water reserve, soil moisture, and the consequent crop production (Srivastava et al. 2014; Praveen et al. 2020). Agrarian-based economies, such as India, where 54% of the workforce is involved in agriculture and allied sectors,

✉ Ankit Tandon
ankittandon@cuhimachal.ac.in

[1] School of Earth and Environmental Sciences, Central University of Himachal Pradesh, Dharamsala, Himachal Pradesh 176215, India

would be highly hit due to the changing rainfall patterns over the Indian subcontinent (Pachauri et al. 2014; Singh et al. 2021). In order to devise sustainable adaptation and mitigation strategies for sustaining agricultural production, water resource management, and overall economy, accurate estimation of variations in rainfall system is a prerequisite. Therefore, it is of great significance to comprehensively examine the ongoing development in the characteristics of current and past variations (temporal evolution) in rainfall patterns by utilizing appropriate methods for evaluation.

Trend analysis is perhaps the most widely used and accepted approach to understand and explore the variability and changes in meteorological parameters (Dash et al. 2007; Sonali and Nagesh Kumar 2013; Westra et al. 2013; Mondal et al. 2015; Karandish et al. 2017; Ay 2020; Dudley et al. 2020; Sharma et al. 2022). Moreover, the analysis also provide insights on the possibility of change tendency of the parameters in the near future (Hamilton et al. 2001; Yue and Wang 2004; Gajbhiye et al. 2016). The most commonly used conventional trend methods are the parametric linear regression (LR) (Haan 1977) and the non-parametric Mann-Kendall (MK) (Mann 1945; Kendall 1948) trend tests, where MK test and Sen's Slope (SS) (Theil 1950; Sen 1968) estimates are often used simultaneously for detecting trend significance and magnitude, respectively. Several studies have been conducted worldwide on trend analysis of various climate parameters by utilizing aforementioned methods (Westra et al. 2013; Karandish et al. 2017; Ay 2020; Dudley et al. 2020). Similarly over Indian domain, numerous studies have been carried out to investigate variability in rainfall patterns and have mostly employed conventional trend methods (Dash et al. 2007; Sonali and Nagesh Kumar 2013; Mondal et al. 2015; Sharma et al. 2022). Although, for long-term trends of rainfall events, MK test performs better than the parametric (LR) tests (Xu et al. 2003) but are sensitive to serial correlations (i.e., persistence) within time series that can lead to overestimation or underestimation of trend significance (Razavi and Vogel 2018). Moreover, the conventional methods are limited for their understanding of changes in the mean representation of a rainfall characteristic and do not provide adequate information about its extreme behavior (Lausier and Jain 2018; Treppiedi et al. 2021). Therefore, these methods are often reported to be less effective for trend detection in extreme rainfall events (Shiau and Huang 2015; Treppiedi et al. 2021). Consequently, despite being widely employed and accepted, conventional trend analysis oftentimes shows inconsistent results (Sanikhani et al. 2018; Birpınar et al. 2023) and is subject to limited information about trends (Uranchimeg et al. 2020; Treppiedi et al. 2021). It is thus become imperative to take on the constraints linked to the conventional approaches and offers an enhanced, accurate, and error-free analysis by employing advanced and modified trend methods.

Most recently, many new non-parametric (Şen 2012; Hassani 2022) machine learning (Darji et al. 2015) and revised and modified (Koenker and Bassett 1978; Hamed and Rao 1998; Şen 2017) trend methods have come to the fore. These methods not only downscale the limitations associated with the classical way of analyzing trends but are also capable of yielding enhanced information about the trends (Güçlü 2018; Treppiedi et al. 2021; Datta and Das 2022). Hence, in previous literature, the implementation of advanced and modified trend methods has enormously improved the accuracy of historical climate trend estimations (Şen 2012, 2017; Mondal et al. 2015; Ahn and Palmer 2016; Malik et al. 2016; Güçlü 2018; Datta and Das 2022; Birpınar et al. 2023). One of the most commonly used modified conventional approach is the modified MK (m-MK) trend test, which eliminates the effect of all autocorrelation coefficients of the time-series by introducing modified variance in classical MK test (Hamed and Rao 1998). This procedure is widely encouraged by numerous researchers around the world for the better trend estimation of climate variables (Hamed 2008; Sonali and Nagesh Kumar 2013; Gajbhiye et al. 2016; Sa'adi et al. 2019). Quantile regression (QR) on the other hand is a powerful and advanced extension of LR, which allows the assessment of changes in different rainfall regimes by estimating slope coefficients of any order (quantile) of the rainfall distribution (Koenker and Bassett 1978). While comparing the parameter regression technique with QR technique for regional flood frequency analysis in Australia, the QR technique performed more accurately for the higher flood percentiles (Haddad and Rahman 2012). Since, QR technique able to distinguish the changes in mean and extreme behavior of a dependent variable, it has been widely employed in the past to study trends at different temporal and spatial levels for rainfall and other climate variables (Choi et al. 2014; Shiau and Huang 2015; Ahn and Palmer 2016; Malik et al. 2016; Gupta et al. 2020; Treppiedi et al. 2021). Nonetheless, majority of studies have predominantly focused on specific distribution quantiles of rainfall parameter. Such restricted outcomes in terms of changes in few specific rainfall regimes fail to provide changes in the entire distribution. While estimating trends across the distribution could be highly beneficial for our understanding of emerging long-term changes in rainfall characteristics. However, over India, the potential of utilizing the QR technique to detect trends and assess trend stability has not been explored. Consequently, there is a need to employ the advanced and modified form of conventional trend methods with the aim, on the one hand, to accurately quantify the historical trends and, on the other hand, to investigate multiple temporal periodicity for explaining temporal evolution and trend stability of rainfall patterns. Thus, the main focus of the present study is to investigate the retrospective rainfall characteristics and associated trends over India by utilizing both modified (m-MK test)

and advanced (QR technique) methods for trend analysis. Moreover, in order to interpret information on temporal evolution and trend stability, the trend patterns across the distribution (using the QR technique) of rainfall characteristics were compared for multiple temporal periods, including the long-term period from 1951 to 2020, the bifurcated periods before and after 1985 (pre-1985 and post-1985), and the most recent period from 2000 to 2020, corresponding to the respective climate zones.

2 Study area and data intake

India is the 7th largest country in the world situated at the southward extension of Asian continent between longitudes 66.5° E–100° E and latitudes 6.5° N–38.5° N. The most prevalent weather phenomena governing the climate of this region are the southwest Indian Summer Monsoons (ISM). ISM mainly occurs during the months of June to September and is capable of distributing ~80% of the total annual rainfall over India (Gadgil 2003). However, the rainfall amount varies enormously in different parts of the country, due to distinct physiographic locations and the distribution and occurrence patterns of ISM rainfall (Mooley and Parthasarathy 1984; Parthasarathy et al. 1994; Dash et al. 2013). For instance, the majority of western and central regions of India experience a rainfall surge of over 90% of their annual precipitation during ISM. Conversely, the southern and northwestern areas receive a rainfall range of 50–75% during this season (Halpert and Bell 1997; Datta and Das 2022). Therefore, the country experiences significant variation in climate conditions, resulting in a high level of spatial variability. Indian Meteorological Department (IMD) has classified the Indian region into six spatially coherent homogenous climate zones viz. Hilly Regions (HR), Northwest (NWI), Central Northeast (CNI), Northeast (NEI), West Central (WC), and Southern Peninsular India (SPI), (Rao 1976). In this study, we considered seven climate zones, as we have separately analyzed HR for Western Hilly Region (WHR) and Eastern Hilly Regions (EHR). Spatial representation of the study area depicting all the considered climate zones along with the altitudinal variations over India is presented in Fig. 1.

The daily gridded rainfall product by IMD, which is available at high (0.25°) spatial resolution over Indian region, has been utilized in the present research. IMD considers a high density rain gauge network of 6995 over India and employs the Inverse Distance Weighted (IDW) interpolation technique to generate high-resolution gridded rainfall dataset (Pai et al. 2014), explained in detail in the source paper by Shepard (1968). Rainfall records for a period of 70 years (i.e., from 1951 to 2020) were extracted from gridded IMD product, and no missing data is encountered in the daily time series.

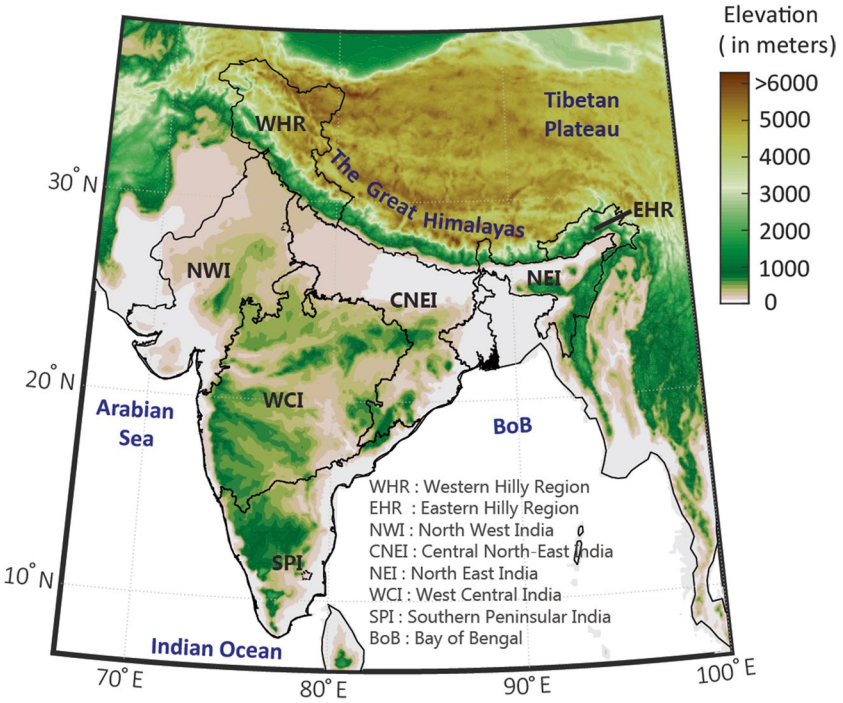

Fig. 1 Study area with topography and climate zones of India in the background. The variations in the elevation ranges from 0 meters to more than 6000 meters above mean sea level. Seven homogeneous climate zones considered in the present study are as follows: Western Hilly region (WHR), Eastern Hilly region (EHR), North West India (NWI), Central northeast India (CNEI), West Central India (WCI), North East India (NEI), and Southern Peninsular India (SPI) of India

3 Methods

3.1 Rainfall characteristics

Rainfall indices play an important role in understanding the rainfall characteristics over any region. Based on the recommendation of Expert Team on Climate Change Detection and Indices (ETCCDI), we have selected six different indices in total, out of which three indices are termed as General Rainfall Characteristics (GRCs) and rest as Extreme Rainfall Characteristics (ERCs). GRCs consist of annual total (Asum) and summer total rainfall (Ssum) as magnitude and number of wet days annually (Nwet) as frequency indices whereas, the ERCs have two magnitudes based on percentiles (P95 and P85) of daily rainfall amount and one daily rainfall intensity (Sdii). The detail classification of all the rainfall indices is presented in Table 1.

3.2 Modified conventional trend approaches

In this study, modified and advanced form of two different conventional trend methods was employed to identify whether trend exists in rainfall characteristics. The first is the modified version of a non-parametric method known as Mann-Kendall (MK) test for identifying trend significance in a time series and Sen's Slope (SS) estimator for the respective trend magnitude. The second trend method employed in this study is an advanced extension of the standard linear regression model known as Quantile Regression (QR). The two procedures are briefly described in the following sections.

3.2.1 Modified Mann-Kendall procedure

The classical MK trend test is a non-parametric trend test (Mann 1945; Kendall 1948) and has been applied in many studies to investigate trend in hydro-climate data series (Sonali and Nagesh Kumar 2013; Singh et al. 2021). In this approach, the differences between each sequential value in a time-series are calculated so as to depict the respective signs through Eq. (1) as follows:

$$signs\left(x_u - x_v\right) = \begin{cases} +1 \; if \; \left(x_u - x_v\right) > 0 \\ 0 \; if \; \left(x_u - x_v\right) = 0 \\ -1 \; if \; \left(x_u - x_v\right) < 0 \end{cases} \tag{1}$$

where "x_u" and "x_v" are values at "u^{th}" and "v^{th}" time instance in time-series with length equals to "n" of a given period. Based on Eq. (1), Kendall sum statistics (S) can be calculated as follows:

$$S = \sum_{v=1}^{n-1} \sum_{u=v+1}^{n} signs\left(x_u - x_v\right) \tag{2}$$

The Kendall statistics S identifies a monotonic trend in the time-series, which assumed to have an asymptotically normal distribution for the sample size $n \geq 8$, with mean $S = 0$ and variance $V(S)$ as follows:

$$V(s) = \frac{n(n-1)(2n+5) - \sum_{p=1}^{m} t_p\left(t_p - 1\right)\left(2t_p + 5\right)}{18} \tag{3}$$

where "m" is the number of tied groups, and "t_p" is the number of values in the p^{th} group.

The basic assumption before employing the MK test is that the time-series have no significant autocorrelations. However, climate variables may have significant autocorrelation in their long-term patterns (Sonali and Nagesh Kumar 2013), which might affect the trend significance of a series. To remove all autocorrelations from the time-series, Hamed and Rao (1998) proposed a revision to the conventional MK test by introducing the modified variance i.e., $mV(s)$, which can be calculated as follows:

$$mV(s) = V(s)\frac{n}{n'} \tag{4}$$

Table 1 List of annual rainfall characteristics used in this study

S.No.	Rainfall indices	Acronym	Description	Unit
1.	GRCs	Asum	Total rainfall amount	mm
2.		Ssum	Total rainfall amount in summer months i.e., June, July, August, and September (JJAS)	mm
3.		Nwet	Number of days with rainfall of 1 mm or more	days
5.	ERCs	P95	95th percentile of daily total rainfall amounts > 1 mm	mm
6.		P85	85th percentile of daily total rainfall amounts > 1 mm	mm
7.		Sdii	Simple daily intensity index i.e., the ratio of Asum and Nwet	mm/ day

Source: Author(s) created

Note: *GRCs* general rainfall characteristics, *ERCs* extreme rainfall characteristics

where $V(s)$ can be obtained from Eq. (3) and $\frac{n}{n'}$ can be calculated as

$$\frac{n}{n'} = 1 + \frac{2}{n(n-1)(n-2)} \sum_{i=1}^{n-1} (n-i)(n-i-1)(n-i-2) r_k \tag{5}$$

where n' is the effective sample size, n is the actual observations, and r_k is the k^{th} lagged significant autocorrelation coefficient of rank k. After evaluating S from Eq. (2) and $mV(s)$ from Eq. (4), a standardized test statistic for MK test i.e., Z statistics was performed to measure trend significance in a time-series. Equation (6) can be used to calculate Z statistics.

$$Z = \begin{cases} \frac{S-1}{\sqrt{V(s)}} \; for \; S > 0 \\ 0 \; for \; S = 0 \\ \frac{S+1}{\sqrt{V(s)}} \; for \; S < 0 \end{cases} \tag{6}$$

The direction of the trend is also indicated by the Z statistics, negative (positive) if decreasing (increasing) trend. In the present study, if the absolute value of Z is greater than 1.96 (at 5% significance level), the null hypothesis of no trend is rejected. Furthermore, to detect trend magnitude, the classical Sen's slope method was used (Theil 1950; Sen 1968). The slope is computed by considering all possible distinct pairs of data values. For N pairs of data, the slope can be calculated as

$$M_i = Median \left[\frac{X_r - X_s}{(r-s)} \right] \forall s < r \tag{7}$$

$$M_{median} = \begin{cases} M_{\left[\frac{N+1}{2}\right]}, & if \; N \; is \; odd \\ \frac{1}{2} \left[M_{\left(\frac{N}{2}\right)} + M_{\left(\frac{N+2}{2}\right)} \right], & if \; N \; is \; even \end{cases} \tag{8}$$

where X_r and X_s are considered as the data values at the corresponding times r and s, respectively. M_{median} value

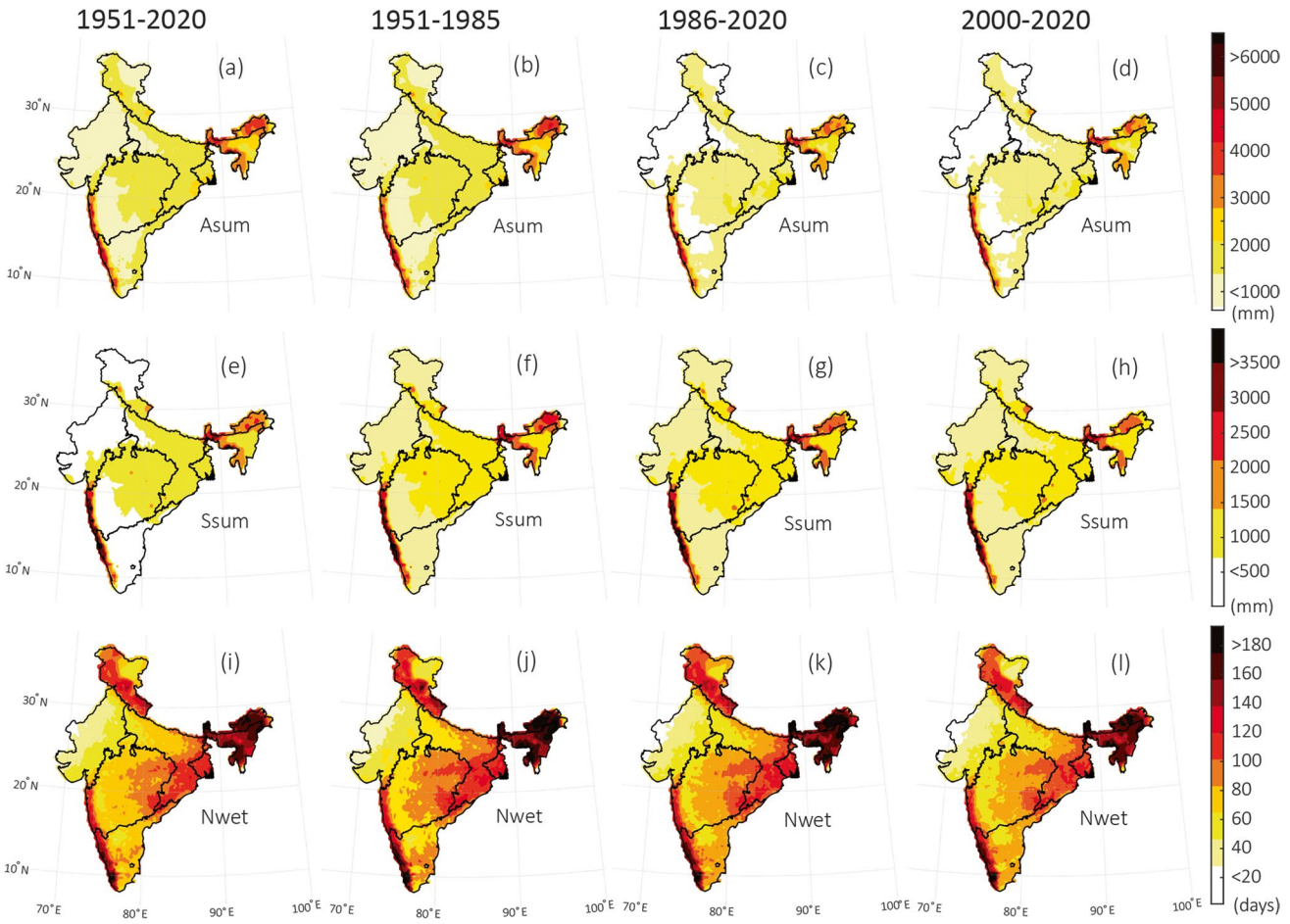

Fig. 2 **a–l** Climatological spatial distribution of GRCs during long-term (1951–2020), bifurcated (pre-1985 and post-1985), and most recent (2000–2020) time periods

indicates the steepness of the trend in the data, whereas its corresponding sign reflects the trend inclination.

3.2.2 Quantile regression (QR) technique

The QR method is first introduced by Koenker and Bassett (1978), to determine the trend at different quantiles (τ). As an advanced extension to the LR, the main advantage of utilizing QR approach is the ability to estimate trends in specific part (quantiles) of the distribution of response variable (Choi et al. 2014). Furthermore, unlike the conventional LR approach that focuses on minimizing the sum of squared errors, QR employs the minimization of a weighted mean of absolute errors (Tareghian and Rasmussen 2013; Konstali and Sorteberg 2022). In standard LR approach, the probability of dependent variable Y in $X = x$ observation, can be expressed as

$$P[Y|x] = A + Bx \tag{9}$$

where A and B are intercept and slope coefficients, respectively of the LR line. While the LR approach concentrates on estimating the average behavior (conditional mean) of a response variable, the QR method is oriented towards identifying conditional quantiles. $0 < \tau < 1$ are the quantile levels, where the central position of the distribution i.e., the median is represented by $\tau = 0.5$. The conditional quantile regression can be expressed as follows:

$$Q_y[\tau|x] = A_\tau + B_\tau X + E_\tau \tag{10}$$

where $Q_y[\tau|x]$ is the expected y for the τ^{th} quantile of x, and A_τ and B_τ are the intercept and slope coefficient of the τ^{th} QR line, respectively, obtained by minimizing the summation of weighted mean of absolute deviations. E_τ is the error with the expectation of zero. A full description of the QR technique can be found in the literature (Koenker and Bassett 1978; Buchinsky 1998; Cade and Noon 2003). In this study, $\tau = 0.1$ (for droughts), 0.5 (for average rainfall), and 0.9 (extreme rainfall) of each rainfall characteristics were considered to estimate A_τ and B_τ at multi-temporal periods. Furthermore, trend in overall distribution of rainfall characteristics i.e., τ values from 0.01 to 0.99 at 0.01 step was also analyzed for each climate zones of

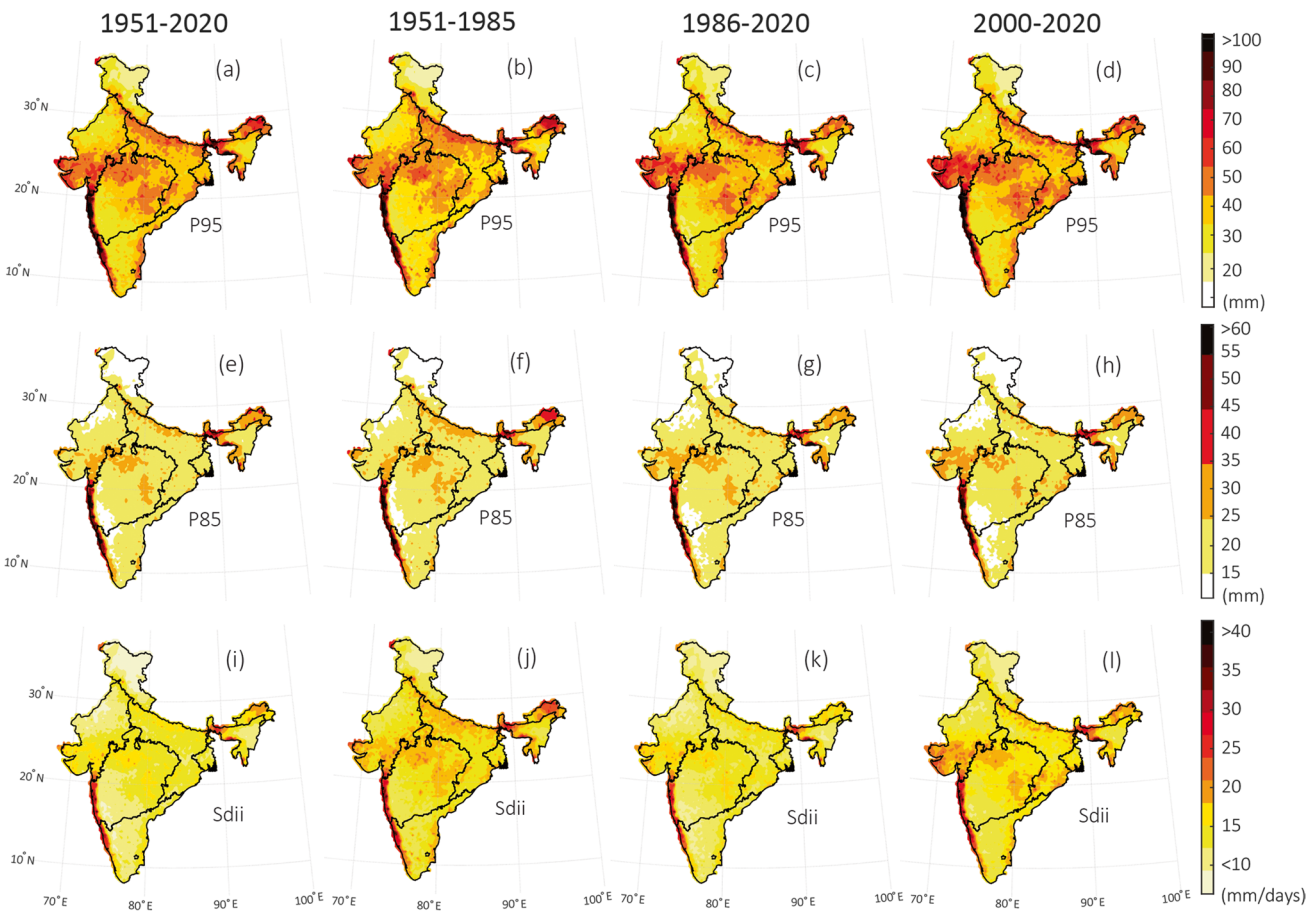

Fig. 3 **a–l** Climatological spatial distribution of ERCs during long-term (1951–2020), bifurcated (pre-1985 and post-1985), and most recent (2000–2020) time periods

India. For trend significance, if the bootstrapped 95% confidence interval around the estimated coefficient for the quantile had overlap with zero, we interpreted this as an indication of a non-significant time trend. This implies the estimated slope coefficients are deemed statistically significant at the 5% significance level when zero lies outside the 95% confidence interval (Laseter et al. 2012; Gao and Franzke 2017).

4 Results and discussion

4.1 Multi-temporal rainfall climatology

In order to determine the climatology of annual rainfall characteristics over India for long-term (19951–2020), bifurcated (pre-1985 and post-1985), and most recent (2000–2020) time periods, we analyzed daily rainfall observations from gridded IMD data for respective time periods. The GRCs and ERCs were then calculated for each grid cell covering the entire Indian region. A detailed summary of the multi-temporal climatology of the respective rainfall characteristics is provided in Sections 4.1.1 and 4.1.2.

4.1.1 General rainfall characteristics

The spatial distribution of GRCs climatology over India in ensemble time average is presented in Fig. 2. The long-term annual total rainfall (Asum) climatology showed high rainfall amount (> 3500 mm) over the Western Ghats of WCI and SPI and also over some portion of EHR and NEI, where most of the rainfall received during ISM (Chatterjee

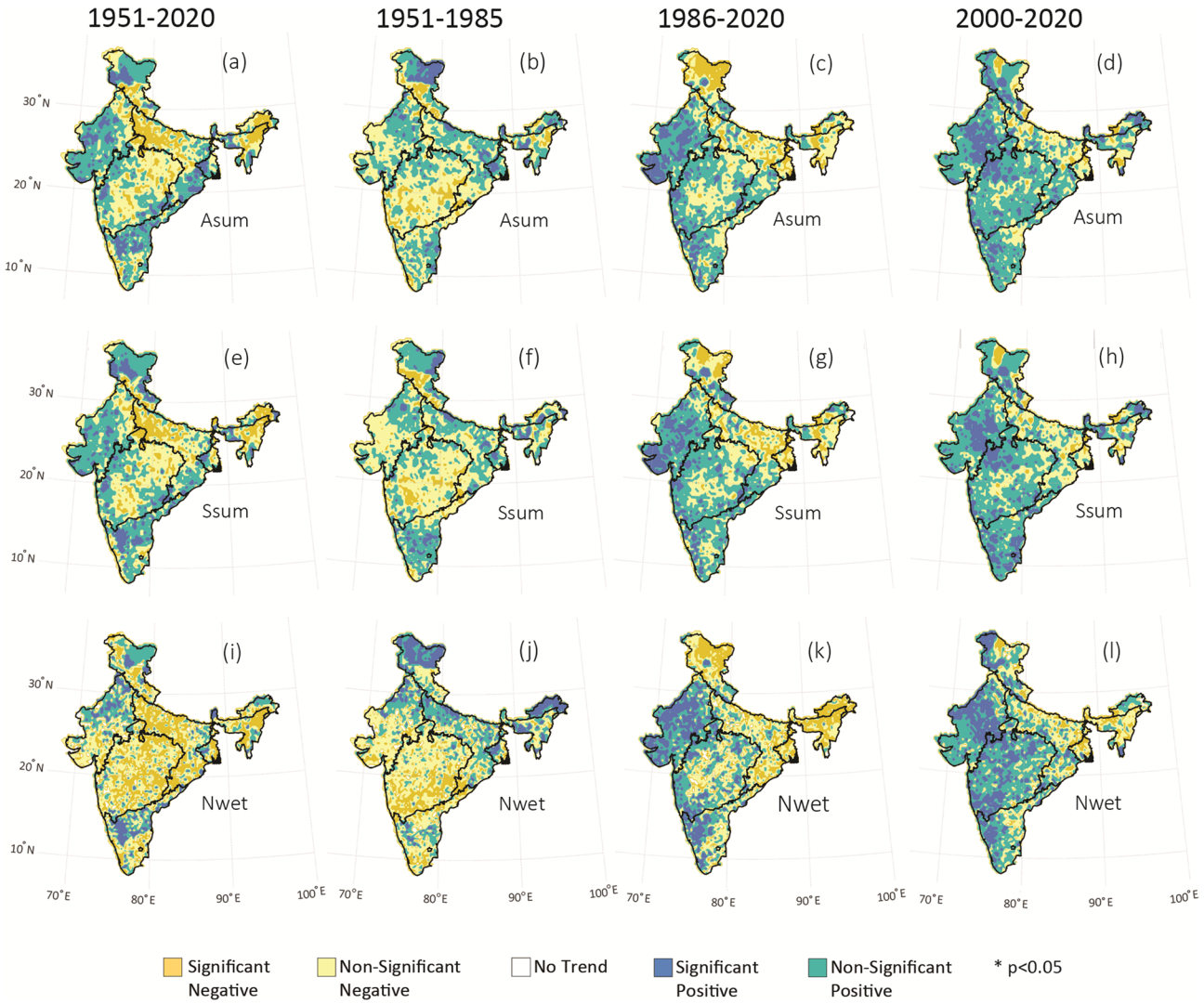

Fig. 4 **a–l** Spatial distribution of trend significance (calculated using m-MK test at $p < 0.05$) in GRCs during long-term (1951–2020), bifurcated (pre-1985 and post-1985), and most recent (2000–2020) time periods

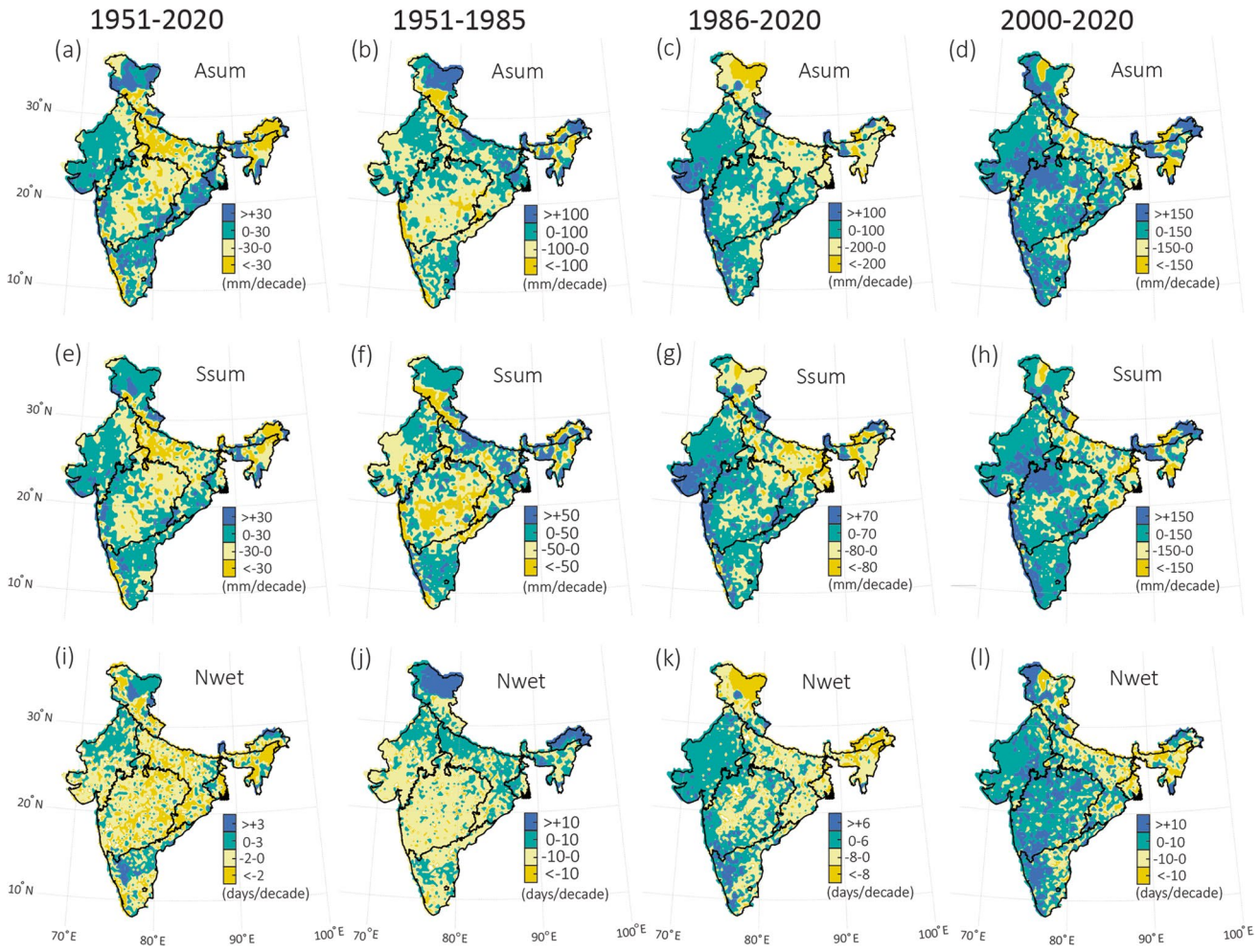

Fig. 5 **a–l** Spatial distribution of trend magnitude (calculated using SS estimator) in GRCs during long-term (1951–2020), bifurcated (pre-1985 and post-1985), and most recent (2000–2020) time periods

et al. 2016; Bhattacharyya and Sreekesh 2022). The moderate Asum (mm) amount (2000 < Asum < 3500) during long-term was mainly observed over WHR, NCI, WCI, and over the Eastern Ghats of SPI climate zones whereas, NWI on the other hand showed comparatively lesser (< 2000 mm) amount of Asum. The bifurcated spatial climatology of Asum on the other hand showed huge discrepancy during pre-1985 and post-1985 time periods. A higher Asum amount over WHR, EHR, CNEI, and SPI climate zones was observed in pre-1985 period as compared to post-1985. This amount was further reduced in the most-recent time period (2000–2020) of respective climate zones. The overall multi-temporal Asum climatology revealed a systematic reduction in the spatial distribution of Asum amount, leading to the drying of Indian climate zones. Similar discrepancies in Ssum climatology over most of the climate zones of India were also observed in long-term and pre-1985 time periods. However, post-1985 and most-recent periods showed higher magnitude of Ssum climatology to that of Asum, especially over the western part of India. Since Indian summer monsoons (ISM) plays a crucial role in distributing around 80% of the total annual rainfall over India (Gadgil 2003; Dash et al. 2013), a lesser Ssum rainfall climatology especially during the long-term period can be the major factor attributing to the overall drying of Indian climate zones. In addition to this, the spatial distribution of Nwet climatology during multi-temporal periods also indicate reduced frequency of rainy days during post-1985 and most-recent time periods. The overall findings from the multi-temporal GRCs climatology conclude that the impact of climate change has led to less frequent and highly variable and spatially heterogeneous rainfall magnitude over Indian climate zones.

4.1.2 Extreme rainfall characteristics

The spatial distribution of ERCs climatology over India in ensemble time average is presented in Fig. 3. The extreme daily rainfall thresholds in "mm" were depicted through P95

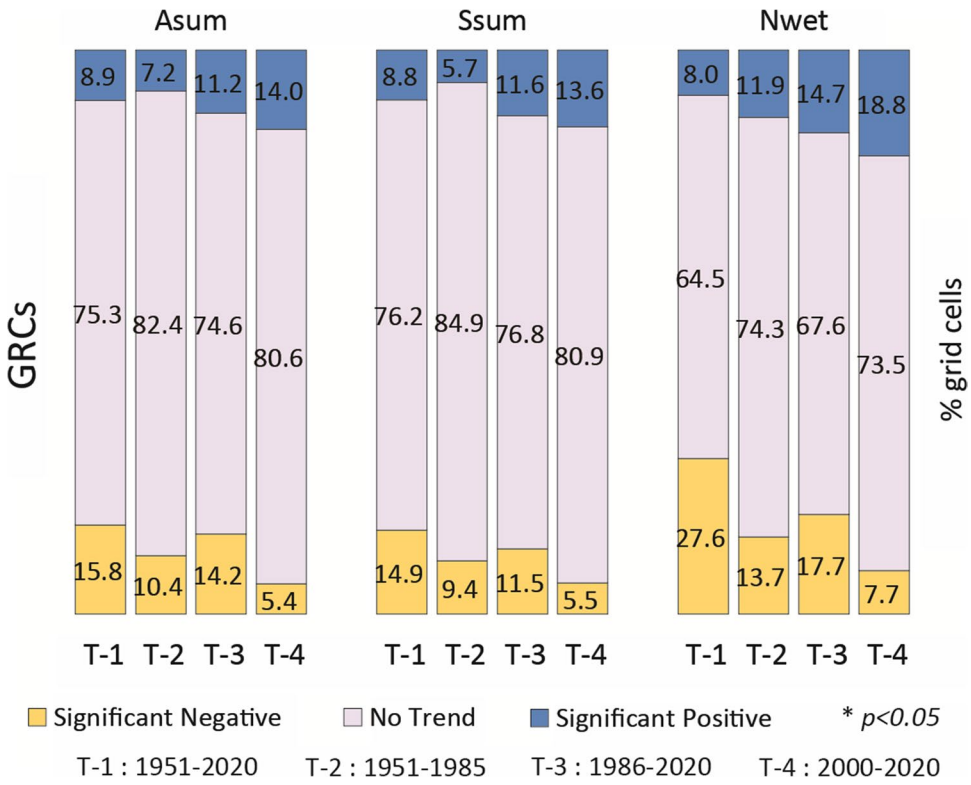

Fig. 6 Percentage of grill cells showing significant positive (blue), significant negative (yellow), and not significant (grey) trend in GRCs using m-MK test at $p < 0.05$. All four temporal periods as T-1 (1951–2020), T-2 (1951–1985), T-3 (1986–2020), and most recent T-4 (2000–2020) aligned together to draw comparison in changing rainfall pattern during different time periods

and P85. Since, the phenomena of intense rainfall over a region are largely governed by topographical features (Wilhite and Glantz 1985; Barros and Lettenmaier 1994; Dimri et al. 2015), a large spatial heterogeneity in the climatological means of ERCs was observed within the topographically variable climate zones. Thus, over Western Ghats, southern NWI, some parts of WHR, NCI, WCI, EHR, and NEI, the long-term average spatial distribution of P95 and P85 showed high thresholds (> 50 mm/day and 25 mm/day, respectively). The intense rainfall over the windward side of Western Ghats and WHR is typically due to the striking of moisture laden winds on the topographic divide which sharply reduces the rainfall on the leeward side (Barros and Lettenmaier 1994; Dimri et al. 2015). Similar phenomena over the EHR, NEI, and NCI climate zones, where the advancing monsoon moisture from Bay of Bengal, resulted in intense rainfall along the foothills, plains, and plateau regions (Singh et al. 2021). The bifurcated climatology of P95 and P85 revealed that the thresholds and spatial extent over NWI, WCI, and NEI have extended, while, the same has reduced over NCI and EHR during the post-1985 period. Contrary to this, the bifurcated climatology of Sdii showed high intensity of daily rainfall during pre-1985 and less intense during post-1985 period. However, the most recent climatology of Sdii showed similar spatial patter to that of extreme thresholds (P95 and P85), indicating enhanced spatial extent of ERCs especially over the western part of India.

4.2 Trends in rainfall using modified Mann-Kendall test

The modified Mann-Kendall (m-MK) test eliminates the effect of autocorrelation in time-series by employing modified variance to generate noteworthy trend existence in time-series. Along with m-MK, SS methodology was also utilized for estimating trend magnitude. Following this, the spatial distribution of the trend significance and magnitude observed in GRCs at multi-temporal periods is illustrated in Figs. 4 and 5, respectively. Furthermore, the percentage of grid cells over the entire Indian region showing significant positive, negative, and no trend for individual GRC is further presented in Fig. 6.

Large heterogeneity in negative and positive trend significance was observed in GRCs in multi-temporal periods. Apparently, all the GRCs showed very similar spatial variations in trend patterns. During long-term, Asum was found significantly decreasing at a rate greater than −30 mm/decade over the large part (15.8%) of the India, including CNEI, NEI, and EHR. The findings of this part are consistent with the findings from the studies of Mondal et al. (2015) and Suthinkumar et al. (2023). The significant increasing trend in Asum on the other hand was limited over few parts of NWI, WHR, and SPI zones. Interestingly, the Asum trends in bifurcated time-series revealed contrasting trend estimations in pre-1985 and post-1985 time periods, elucidating the

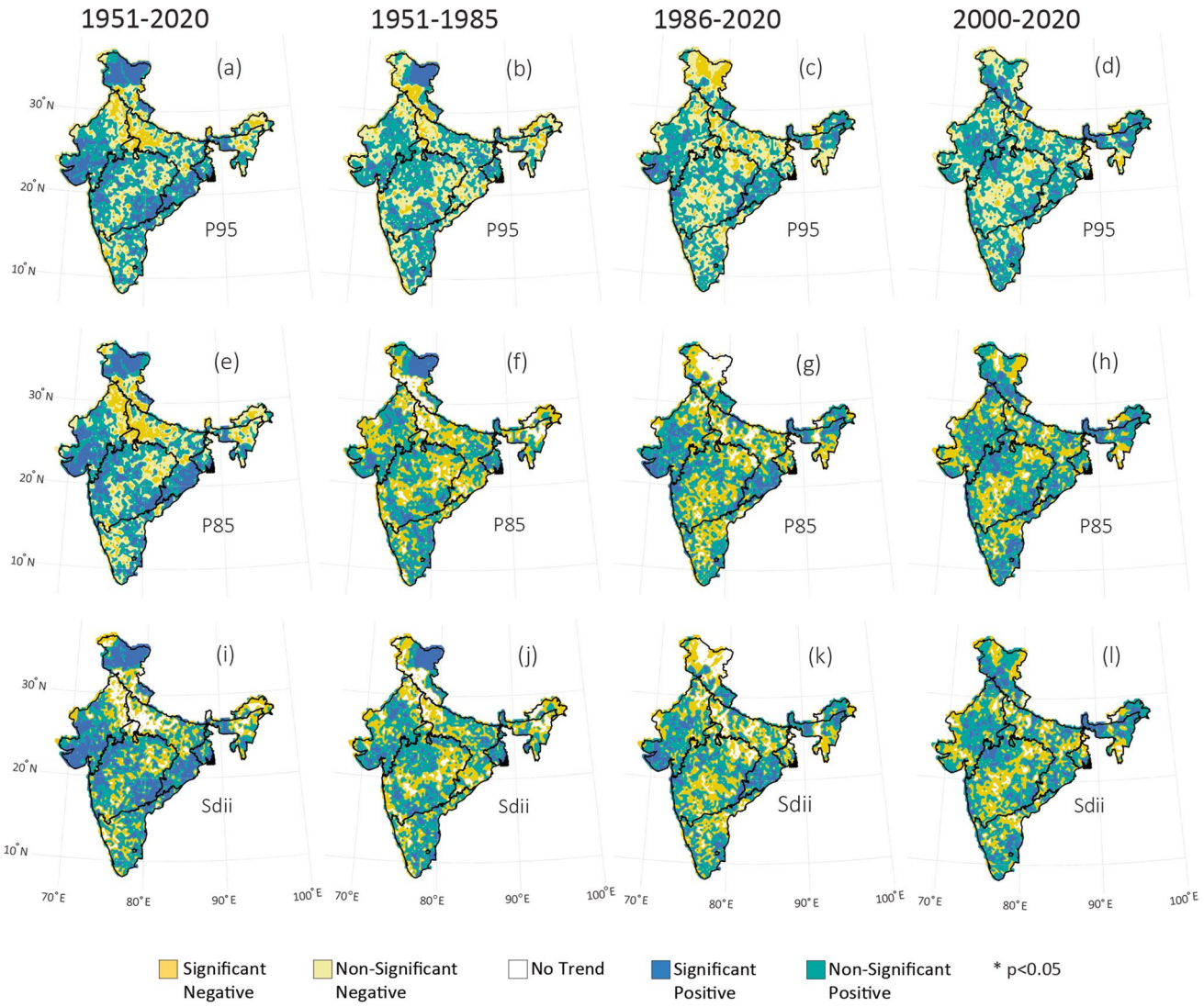

Fig. 7 **a**–**l** Spatial distribution of trend significance (calculated using m-MK test at $p < 0.05$) in ERCs during long-term (1951–2020), bifurcated (pre and post-1985), and most recent (2000–2020) time periods

clear remarks of climate change across the climatic zones of India. The most vulnerable climate zones exhibiting a completely reversed Asum trends in pre-1985 and post-1985 periods were NWI, WHR, WCI, CNEI, and NEI. Whereas, during the most-recent time period, the entire western part of the Indian region encompassing 14% of the India showed significant positive trend, and mere 5.4% of grid cells showed significant negative trend in Asum. More or less similar trend patterns of Asum and Ssum were observed, while the frequency characteristic (Nwet) showed much stronger evidence of long-term drying and recent enhancement of rainfall over the Indian climate zones. Since ISM provides most of the rainfall across India, the overall variations in GRCs can be attributed to the intricate nature and nonlinear characteristics of the ISM, which often shows variabilities ranging from intraseasonal to multidecadal (Varikoden and Babu 2015; Hrudya et al. 2020). The high and low rainfall on the account of active and break phases, respectively, is subjected to the intraseasonal variability (Ramamurthy 1969; Gadgil 2003; Rajeevan et al. 2010), while the sea surface temperature (SST) anomalies in both Atlantic and southwest Pacific regions are associated with the multidecadal variability in ISM character (Joseph et al. 2013; Varikoden and Babu 2015). Consequently, the overall drying of CNEI, WCI, and NEI zones can be associated with the persistent break phase (Ramesh Kumar et al. 2009; Mondal et al. 2015). Whereas, significant rise during post-1985 and most-recent time periods can be associated with ISM multidecadal variabilities. The most robust sources of ISM rainfall predictability during JJAS are the El Niño Southern Oscillation (ENSO) and the snowfall across the Himalayas (Shukla and Wallace 1983; Kripalani et al. 2003; Annamalai

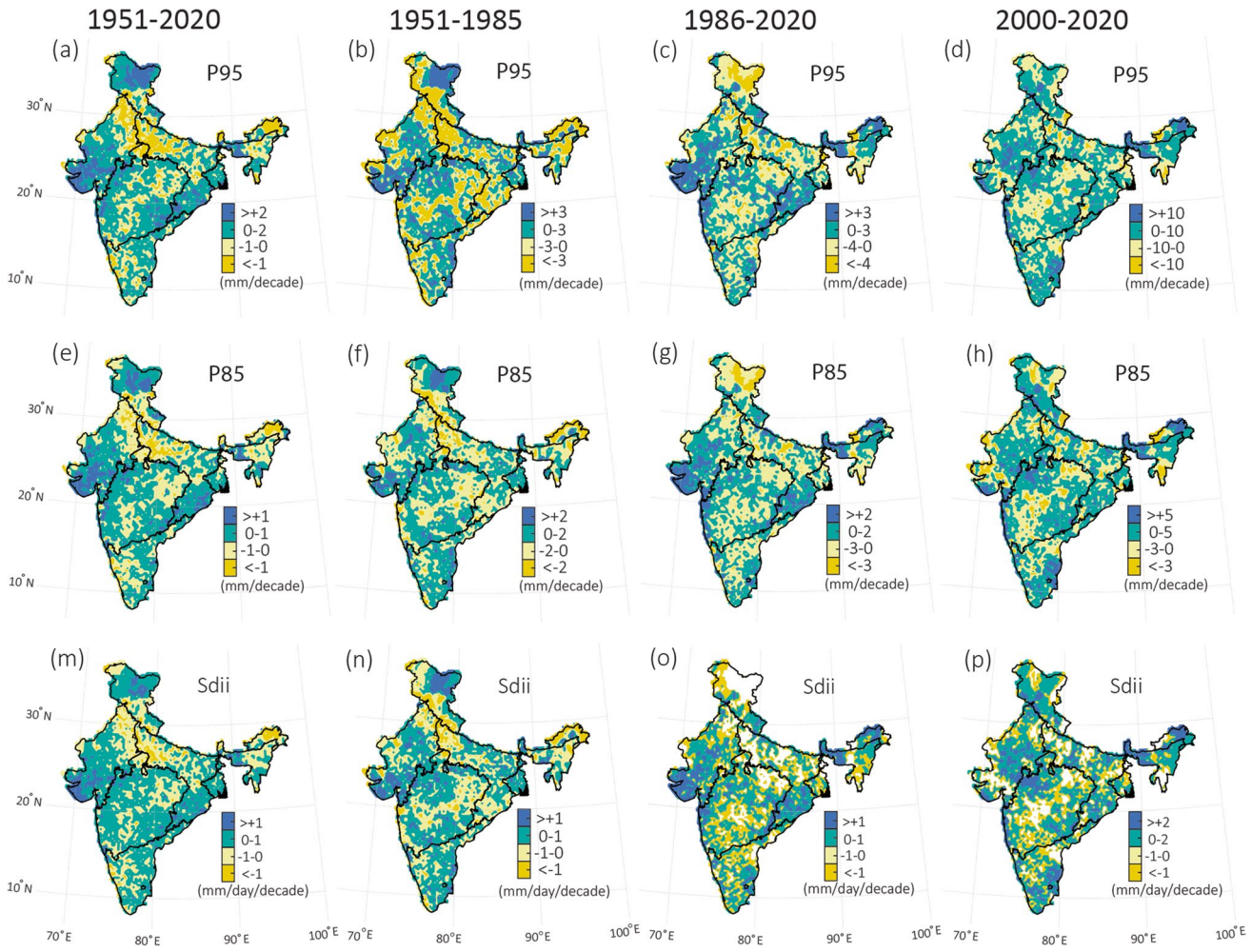

Fig. 8 **a–l** Spatial distribution of trend magnitude (calculated using SS estimator) in ERCs during long-term (1951–2020), bifurcated (pre and post-1985), and most recent (2000–2020) time periods

et al. 2007; Ashok and Saji 2007). The El Niño accounts for the deficit in rainfall amount, while the La Niña is responsible for the surplus rainfall over India whereas, the less winter snowfall over the Himalayas provides favorable monsoon conditions and vice-versa (Kripalani et al. 2003). Although, the interconnected land-ocean-atmospheric processes greatly affect the monsoonal trends and rainfall characteristics, but these also pose significant challenges in comprehending the fundamental mechanisms at play, owing to their complex nature (Ramesh Kumar et al. 2009; Mondal et al. 2015).

Similar to GRCs, the spatial distribution of trend significance and magnitude in ERCs at multi-temporal period is illustrated in Figs. 7 and 8, respectively. The percentage of grid cells over the entire Indian region showing significant positive, negative, and no trend for individual ERC is presented in Fig. 9 although the multi-temporal changes in magnitude (P95 and P85) and intensity (Sdii) of ERCs were observed to have very similar spatial patterns, but are subject to huge variability in extreme rainfall trend patterns over different climate zones. During long-term period, the climate zones including WHR, NWI, WCI, and southern CNEI were observed to have positive trend in ERCs, while the northern CNEI, NEI, EHR, and SPI climate zones majorly showed negative trend. In particular, P95, P85, and Sdii showed significant positive trend over the large (19.7%, 19.5%, and 23.1%, respectively) part of India, while significant negative trend was limited for few (11.8%, 14.7%, and 13.8%, respectively) regions over India. However, very less significant trends in ERCs over India were observed during bifurcated and most-recent time period. Despite that, the positive trends in ERCs, especially along the western part of the Indian region could be primarily associated with the intense heating of the Arabian Sea and tropospheric warming due to climate change, which results in frequent advection of low-level jet stream towards the continent (Konwar et al. 2012; Roxy et al. 2017; Xavier et al. 2018; Varikoden et al. 2019). Furthermore, the increased frequency (~52%) of tropical cyclone over the Arabian Sea and decreased

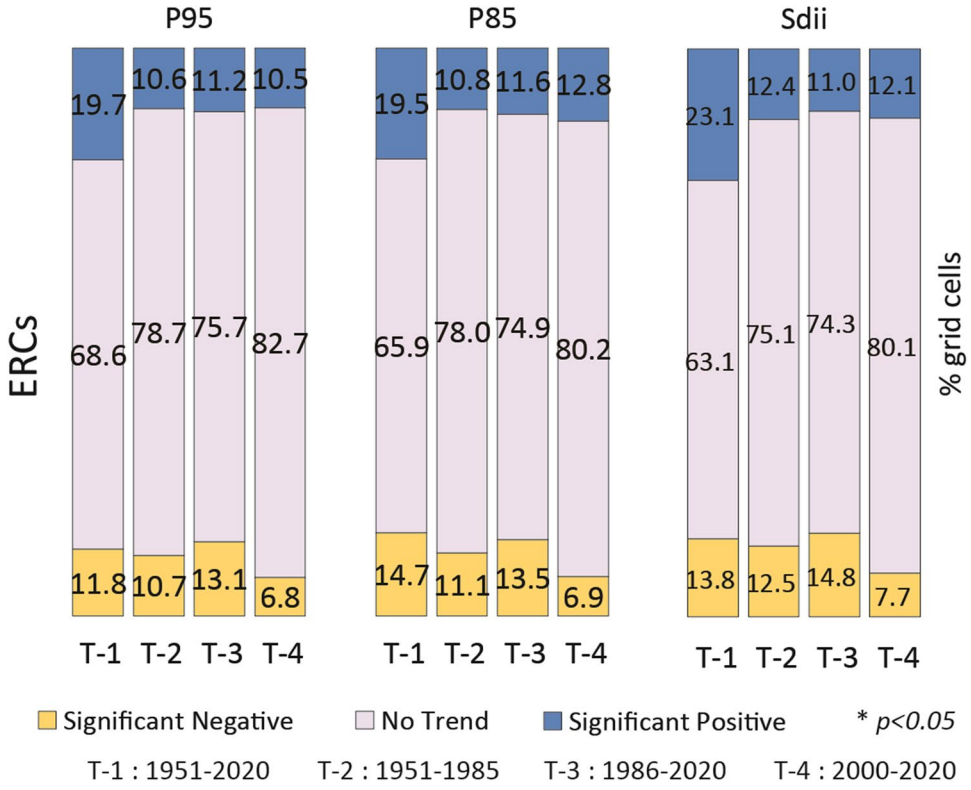

Fig. 9 Percentage of grill cells showing significant positive (blue), significant negative (yellow), and not significant (grey) trend in ERCs using m-MK test at $p < 0.05$. All four temporal periods as T-1 (1951–2020), T-2 (1951–1985), T-3 (1986–2020), and most recent T-4 (2000–2020) aligned together to draw comparison in changing rainfall pattern during different time periods

frequency (~8%) over the Bay of Bengal during 2001-2019 can explain the observed trend heterogeneity in ERCs over India in most-recent time period (Deshpande et al. 2021). It is interesting to note that the rate, at which P95 was reported to change over these locations, was almost twice the rate of change of P85, indicating higher vulnerability to very wet extremes. Overall, the multi-temporal variations in GRCs showed opposite trend components to that of ERCs over India although the long-term trends of GRCs showed drying pattern, but a consistent increment was also reported from pre-1985 to post-1985 and most-recent time periods. Contrastingly, the long-term trends of ERCs showed significant increasing trend, while less trend significance was reported for ERCs during pre-1985, post-985, and most-recent time periods. Altogether, the frequency and intensity rainfall characteristics showed highest variability in trend significance across Indian climate zones.

4.3 Trends in rainfall distribution using quantile regression technique

A modern regression approach known as quantile regression (QR) was employed to estimate the variability in different parts (quantiles) of the rainfall distribution. The QR method was applied to both GRCs and ERCs for long-term, bifurcated, and most-recent temporal periods. The results of the spatial distribution of trends in GRCs and ERCs at different quantiles ($\tau = 0.1$, 0.5, and 0.9) are summarized in the first subsection. Subsequently, a subsection focuses on the analysis of trends in quantiles ($\tau = 0.01$ to 0.99) distribution of rainfall characteristics over different climate zone during multiple temporal periods. This investigation aims to understand how the trends in rainfall characteristics across Indian climate zones have changed in terms of evolution and consistency over time, taking into account the long-term, bifurcated, and most-recent periods.

4.3.1 Spatial distribution of rainfall trends at lower, middle, and upper quantiles

Figures 10 and 11 depict the significance of long-term trends in the lower ($\tau = 0.1$), median ($\tau = 0.5$), and upper ($\tau = 0.9$) quantiles of GRCs and ERCs, respectively. The corresponding trend magnitudes are illustrated in Fig. 12 for GRCs and Fig. 13 for ERCs. Notably, the Asum rainfall exhibited a significant positive change in trend direction, particularly in the WHR climate zone, where the spatial extent increased significantly from the lower quantile ($\tau = 0.1$) to the upper quantile ($\tau = 0.9$). This indicates the regional vulnerability towards more extreme rainfall events. Similar patterns were observed in the SPI and certain areas of the Western Ghats. Conversely, the CNEI, NWI, and EHR displayed negative trends in the middle and extreme distribution of Asum characteristics. However, during the most recent time period, a

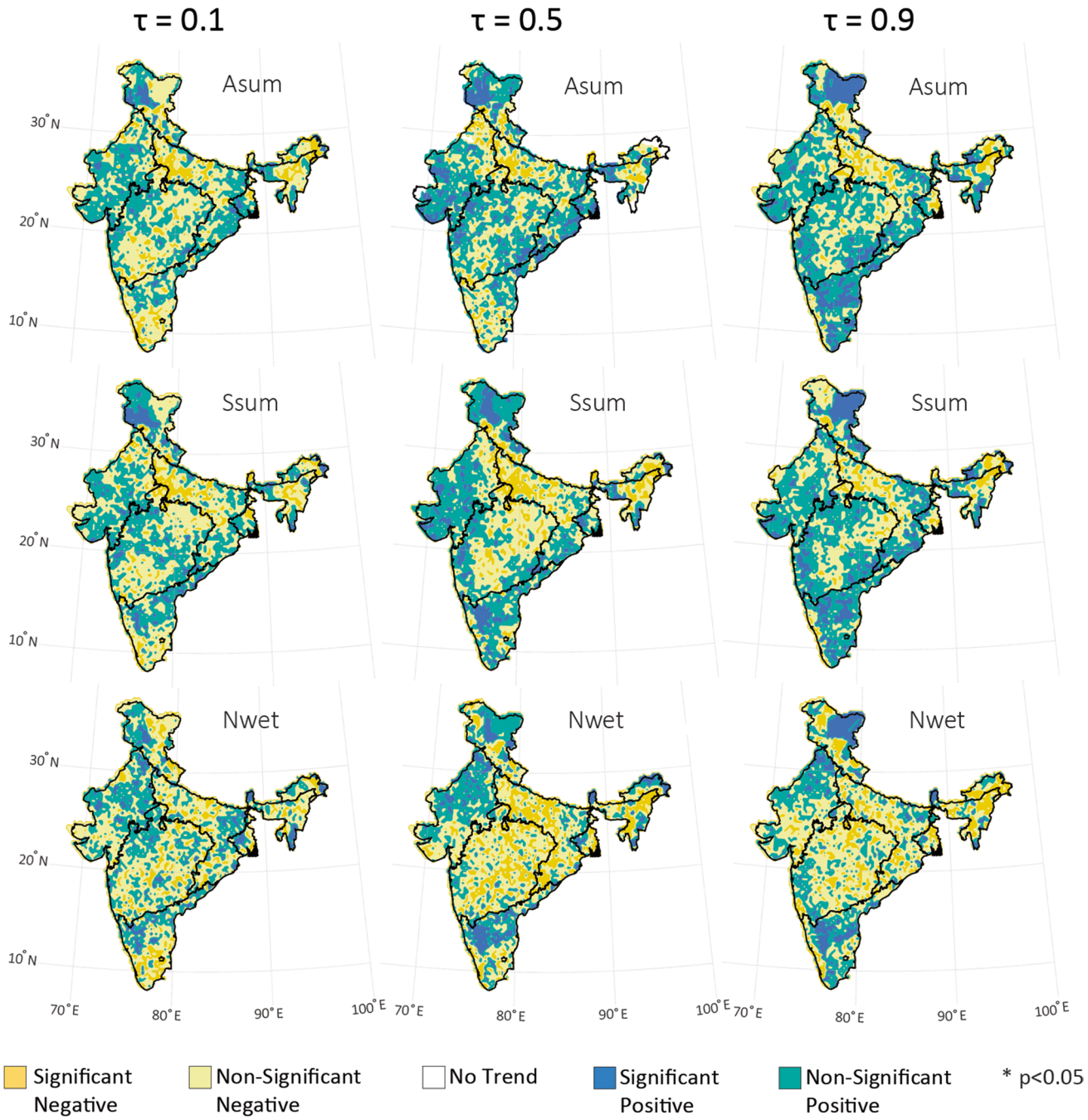

Fig. 10 Spatial distribution of long term (1951–2020) trend significance (negative/positive) in GRCs (at $p < 0.05$, using QR approach) at three different quantile levels; lower ($\tau = 0.1$), middle ($\tau = 0.5$), and upper ($\tau = 0.9$) tails of the respective rainfall characteristic distribution

majority (16%) of the study region exhibited a significant increase in both the upper ($\tau = 0.9$) and lower ($\tau = 0.1$) tail distribution of Asum. This is presented in Fig. 14, which demonstrates the percentage of significant regions in India with negative and positive trends in GRCs distribution during the multi-temporal period. The corresponding percent area contribution of ERCs trend significance over India is illustrated in Fig. 15. Given that areas with high variability in rainfall patterns are more prone to droughts and extreme floods (Pandey and Ramasastri 2001; Gajbhiye et al. 2016), the observed changes in this study directly indicate recent intensification in both extreme floods and droughts across Indian climate zones. Similar spatio-temporal changes were observed in the Ssum rainfall characteristic across the lower, middle, and upper tails. It is noteworthy that the regions exhibiting positive changes in the upper tails have

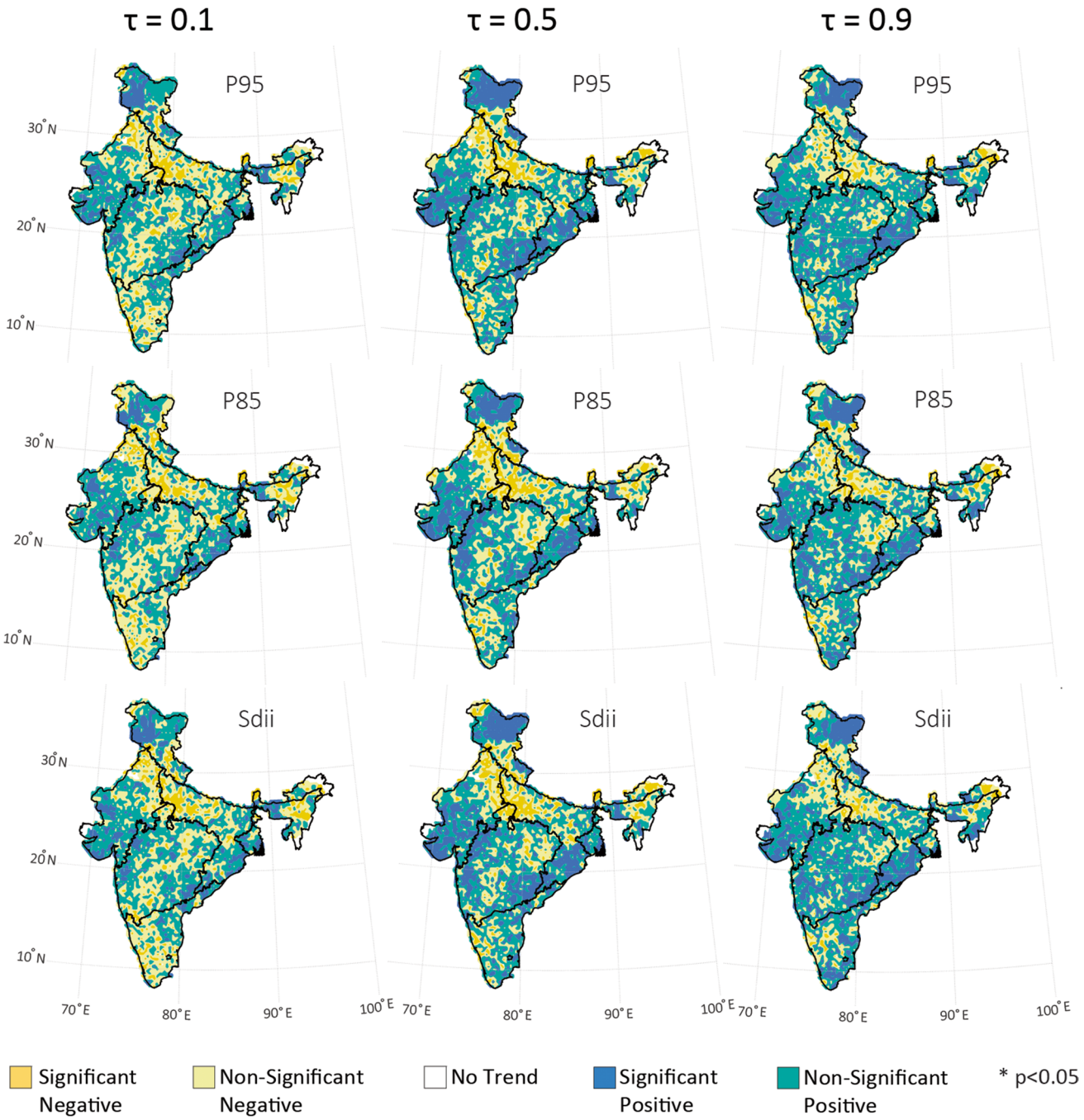

Fig. 11 Spatial distribution of long term (1951–2020) trend significance (negative/positive) in ERCs (at $p < 0.05$, using QR approach) at three different quantile levels; lower ($\tau = 0.1$), middle ($\tau = 0.5$), and upper ($\tau = 0.9$) tails of the respective rainfall characteristic distribution

not only doubled in spatial extent but also doubled in magnitude compared to the lower tail distribution (Figs. 12 and 13). These findings align with the research by Ghosh et al. (2016), which highlighted significant spatial variability in trends between mean and extreme rainfall events in India. Furthermore, it was observed that the trends in the lower tail distribution of most rainfall characteristics indicate severe drought conditions in the WCI, CNEI, and some parts of NEI. These long-term trends are consistent with the findings of Malik et al. (2016), where the lower tail distribution was considered representative of droughts. This drying trend was also evident in the Nwet characteristic at median distribution, where approximately 23% of the Indian region exhibited a significant negative trend during the long-term period. However, the post-1985 and most recent time periods indicated a significant increase in Nwet days across the entire

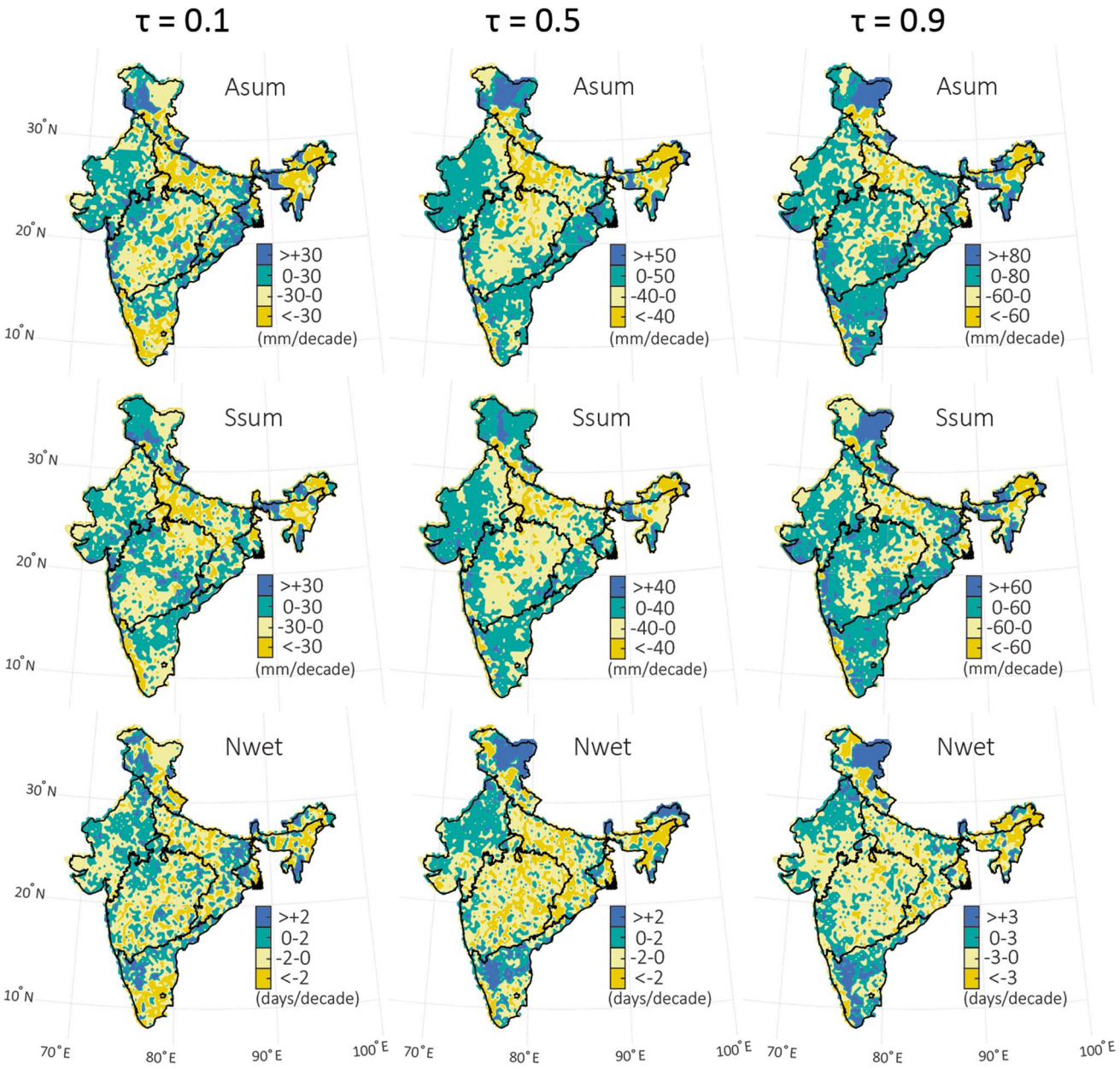

Fig. 12 Spatial distribution of long term (1951–2020) trend magnitude (negative/positive) in GRCs (using QR approach) at three different quantile levels; lower ($\tau = 0.1$), middle ($\tau = 0.5$), and upper ($\tau = 0.9$) tails of the respective rainfall characteristic distribution

distribution. Furthermore, during the long-term period, the middle ($\tau = 0.5$) and upper ($\tau = 0.9$) tails of ERCs showed significant increment over a large portion of the Indian landmass, which had less significance in the bifurcated and most recent periods.

4.3.2 Trend stability and evolution in rainfall distribution

Given the distinct disparities observed in the long-term (1951–2020) patterns of rainfall characteristics when compared to the bifurcated (pre-1985 and post-1985) and most recent (2000–2020), the present analysis allows for the identification of trend stability and evolution. According to the recommendations put forth by Güçlü (2018), the presence of a consistent trend component across both the complete (i.e., 1951–2020 in our study) and partial (i.e., pre-1985 and post-1985 in our study) time series implies trend stability, whereas any discrepancies indicate instability. In order to ensure trend stability across diverse climate zones for various rainfall characteristics, we calculated the vector of coefficients for area-averaged time series for multiple time periods and quantile levels ranging from $\tau =$

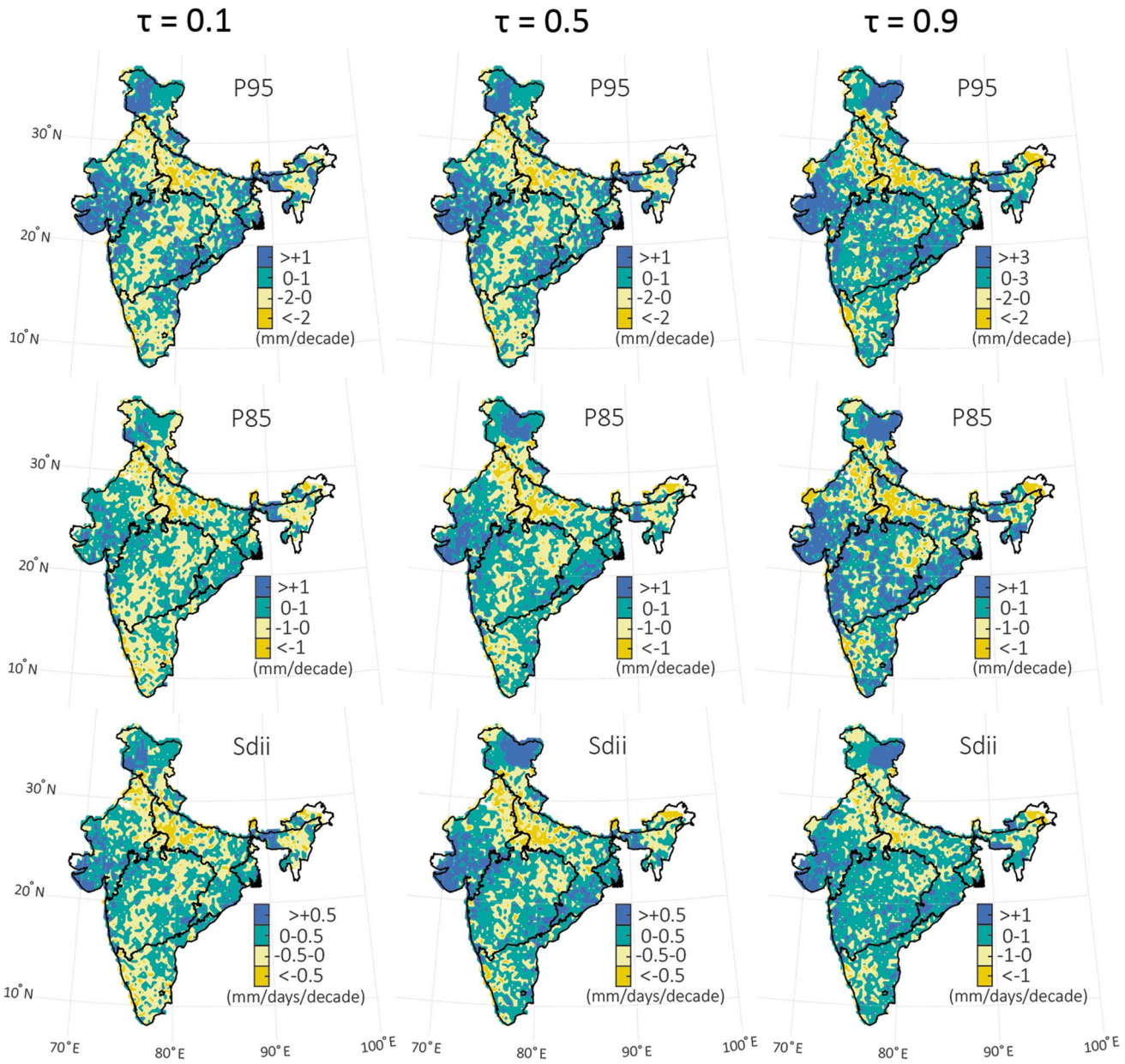

Fig. 13 Spatial distribution of long term (1951–2020) trend magnitude (negative/positive) in ERCs (using QR approach) at three different quantile levels; lower ($\tau = 0.1$), middle ($\tau = 0.5$), and upper ($\tau = 0.9$) tails of the respective rainfall characteristic distribution

0.01 to 0.99 (in 0.01 steps). The slope coefficients at varying quantiles ($\tau = 0.01$ to 0.99) of rainfall characteristics i.e., Asum, Ssum, Nwet, Sdii, P95, P85, N10, and N20 at multi-temporal time periods are presented in figures from Figs. 16, 17, 18, 19, 20, and 21, respectively. Through an examination of the slope coefficients associated with different rainfall characteristics during the considerate temporal periods across various quantiles, it becomes feasible to draw inferences regarding the fluctuations in trend magnitude throughout the entirety of the rainfall distribution. Moreover, its comparison at multi-temporal periods also elucidates information on the temporal evolution and trend stability of rainfall characteristics over respective climate zone. It is essential to emphasize that the most recent time period has witnessed a substantial escalation in both the range and magnitude of these slope coefficients whereas, in the context of the long-term period, particularly within the WHR climate zone, it was observed that as the conditional quantile level of rainfall characteristics increases, so does the corresponding value of the slope coefficient. This growth was particularly significant at extremely high quantile levels (i.e., $\tau > 0.8$). However, distinct trends in

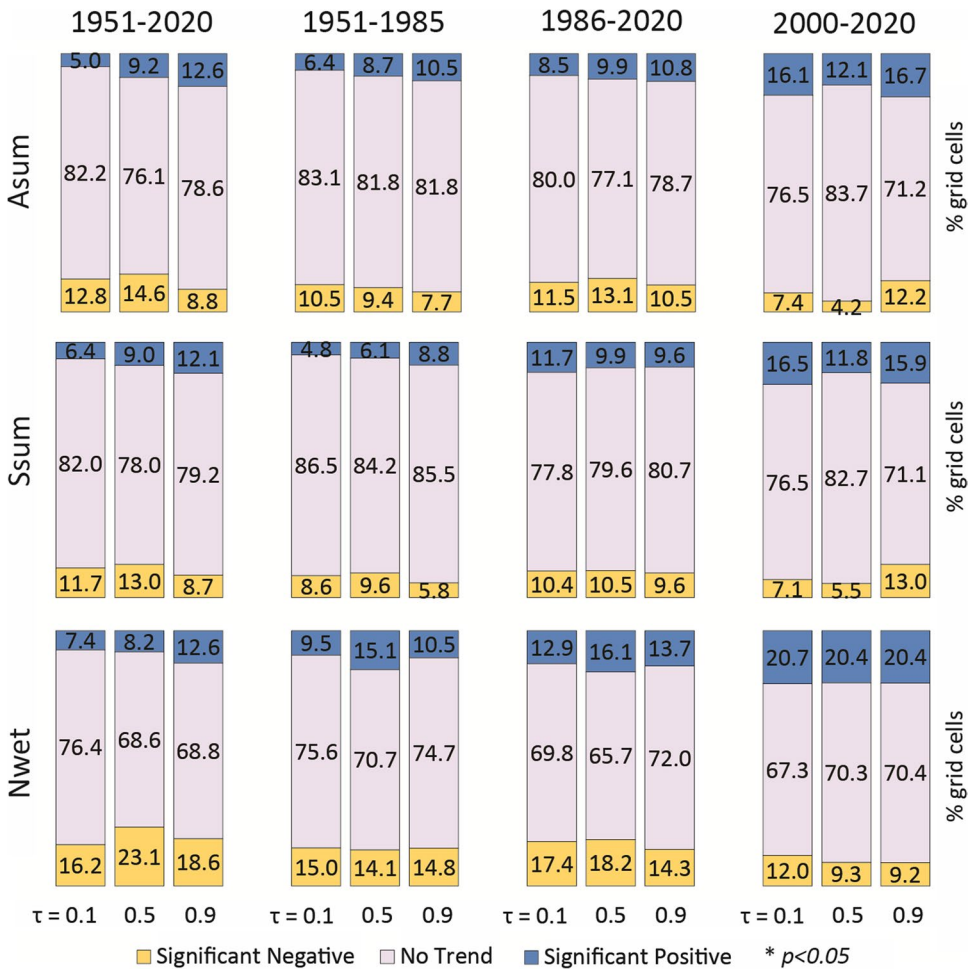

Fig. 14 Percentage of grid cells showing significant positive (blue), significant negative (yellow), and non-significant (grey) trends in GRCs at multi-durational time periods over the entire India. Trends in each time duration characterized for lower ($\tau = 0.1$), middle ($\tau = 0.5$), and upper ($\tau = 0.9$) tails, to represent the underline changes in extreme and mean behavior of rainfall indices using QR

rainfall distribution were observed during the pre-1985 and post-1985 time periods. The pre-1985 period exhibited a predominance of positive trends, while the post-1985 epoch displayed a contrasting prevalence of negative trends. Furthermore, in the most recent time period, the slope coefficient demonstrated significant negative values at exceptionally high quantile levels. Consequently, it can be inferred that the trends in rainfall distribution across the WHR are highly unstable. A similar pattern of rainfall trend instability was also observed across the EHR climate zone. However, in the long-term and post-1985 periods, a majority of rainfall characteristics exhibited significant negative trends in both the lower and higher tails. The instability in trend over EHR zone was further followed by the most recent period, where extremely wet rainfall (P95) displayed significant positive trends at very high quantile levels ($\tau > 0.8$). The neighboring NEI zone exhibited comparable variability in rainfall distribution, except for the intense (Sdii) and extreme wet (P95) conditions evident in their long-term pattern. Most of the rainfall characteristics across the NWI, CNEI, SPI, and WCI zones displayed non-significant but stable trends across the entire quantile distribution. However, certain rainfall characteristics such as Sdii, P95, and P85 exhibited significant positive trends in these climate zones, particularly at higher quantile levels. For instance, in the SPI climate zone, rainfall frequency (Nwet) along with magnitude (Asum, Ssum) demonstrated significant growth at high quantile levels during the post-1985 and most recent periods. Overall, the variability of rainfall across the climate zones of India highlights that the extreme segments of the distribution are undergoing significant changes in conjunction with temporal evolution. Furthermore, the consistencies in rainfall trends across different climate zones exhibit substantial variability and mainly credited to the strength and weakening of ISM rainfall (Vidya et al. 2020). Several large-scale climate forcings (such as ENSO, Madden-Julian Oscillation, and Indian Ocean Dipole etc.) and anthropogenic forcings influencing ISM rainfall might be attributed to the

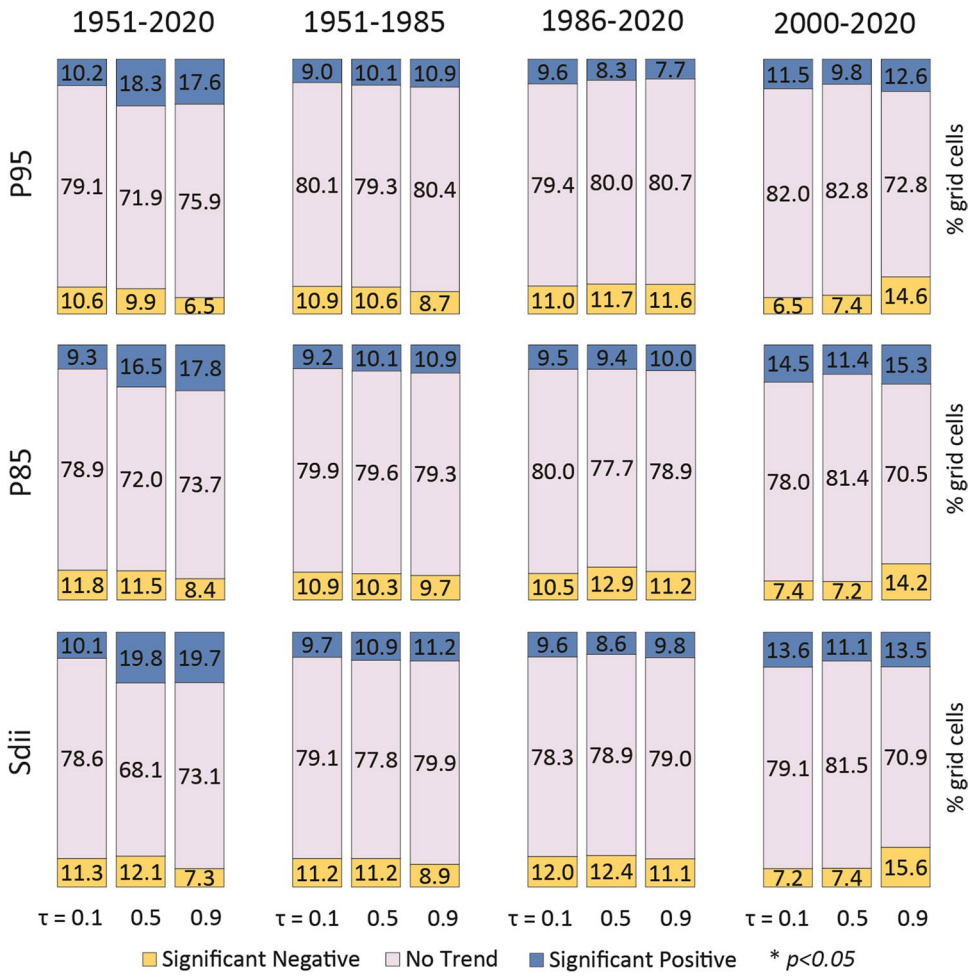

Fig. 15 Percentage of grid cells showing significant positive (blue), significant negative (yellow), and non-significant (grey) trends in ERCs at multi-durational time periods over the entire India. Trends in each time duration characterized for lower ($\tau = 0.1$), middle ($\tau = 0.5$), and upper ($\tau = 0.9$) tails, to represent the underline changes in extreme and mean behavior of rainfall indices using QR

observed instabilities in rainfall trends over Indian climate zones (Singh et al. 2019; Das et al. 2020).

4.4 Conclusion

In this study, a comprehensive assessment of multi-temporal variability in rainfall characteristics over Indian climate zones was carried out for long-term (1951–2020), bifurcated (pre-1985 and post-1985), and most-recent (2000–2020) time periods. Trends in six different rainfall characteristics of GRCs and ERCs were evaluated using advanced (QR) and modified (m-MK) conventional methods. It is evident from the implemented methods that the variations in trends over Indian climate zones differ with respect to the different temporal periods. During long-term period, trends in GRCs exhibited drying patterns, while opposite increasing trends were observed in ERCs for most of the study region. Whereas during bifurcated time periods, a contrasting trend of rainfall characteristics were observed over most of the climate zones including NWI, WHR, WCI, CNEI, and NEI showing clear remarks of climate change across these zones. Furthermore, during most-recent time period, the entire western part of India showed significant positive trend in GRCs (~16%) and ERCs (~12%), while comparatively very small region showed significant negative trend in GRCs (~6%) and ERCs (~7%), thus indicating recent intensification of rainfall over India. While considering the multi-temporal evolution from pre-1985 to post-1985 and most-recent time periods, a systematic increment was reported in percent region showing significant positive trends of GRCs. On the other hand, with respect to ERCs, only the long-term variations showed majority of significant trends, while the bifurcated and most-recent time periods showed comparatively less significant trend. It is interesting to note that despite no such evolution in significant positive trend of ERCs, a remarkable reduction (~50%) in percent region showing significant negative trends was observed while comparing post-1985 and most-recent periods. Altogether, the trend estimates from m-MK test were found more or less consistent with the results of QR at median tail ($\tau = 0.5$)

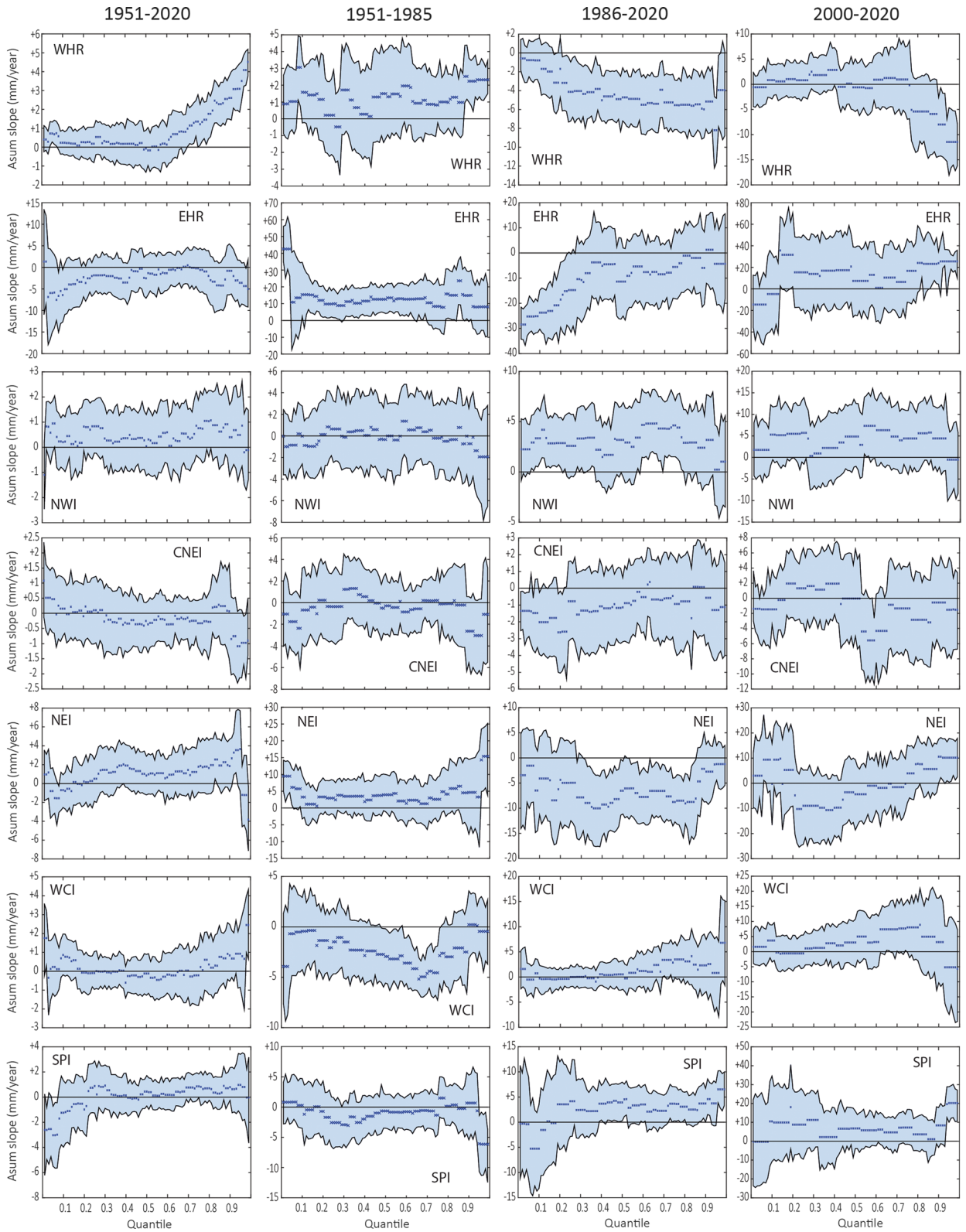

Fig. 16 Multi-temporal slope coefficient of annual total rainfall (Asum) regression line at different quantile levels (τ = 0.01–0.99). Blue points are representative of the slopes for various quantiles, black line represents zero slope i.e., no change and light blue area stands bootstrapped upper and lower 95% confidence intervals. Rows depicting different climate zones of India, while columns display long-term (1951–2020), pre-1985 (1951–1985), post-1985 (1986–2020), and most-recent (2000–2020) time periods

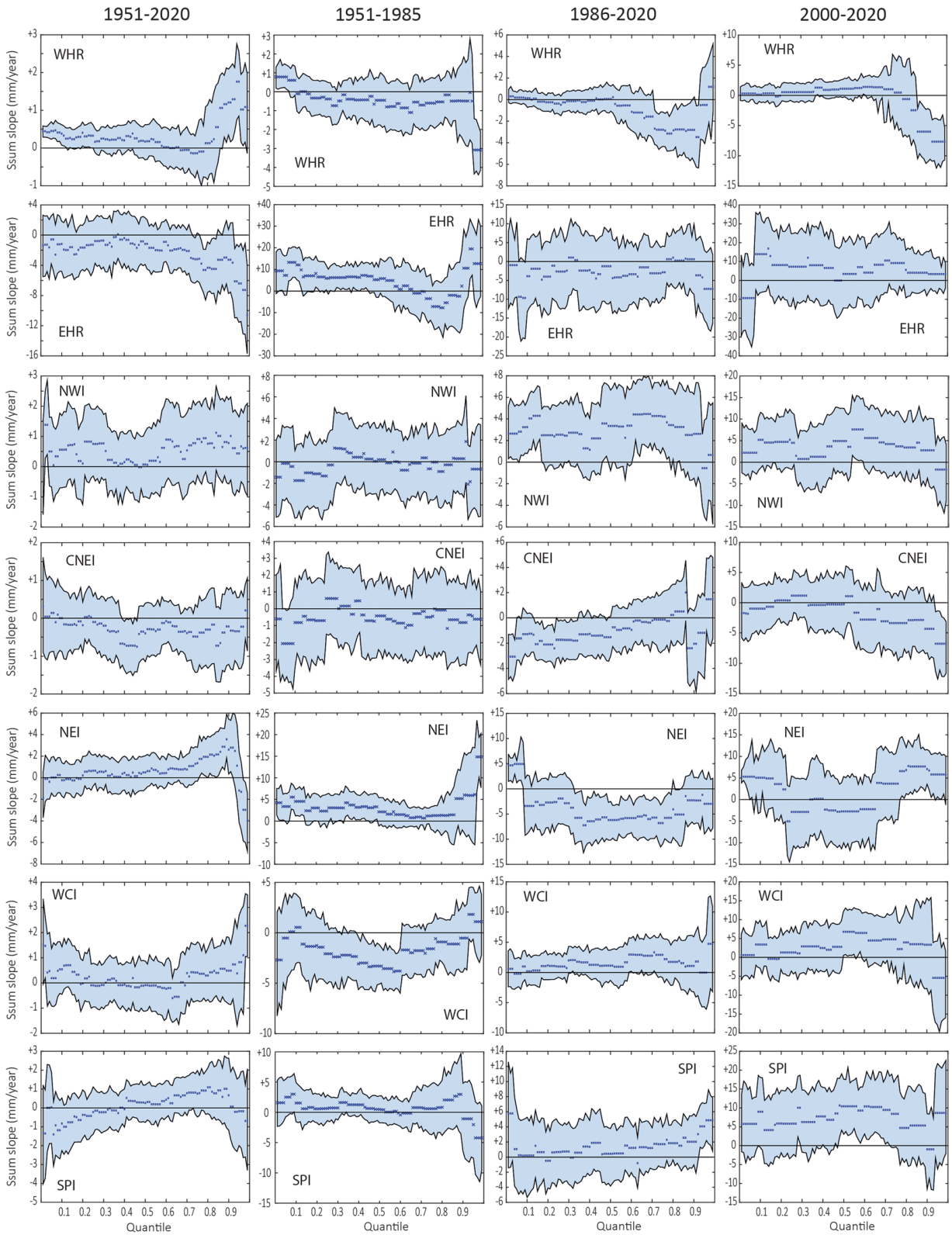

Fig. 17 Multi-temporal slope coefficient of summer total rainfall (Ssum) regression line at different quantile levels (τ = 0.01–0.99). Blue points are representative of the slopes for various quantiles, black line represents zero slope i.e., no change and light blue area stands bootstrapped upper and lower 95% confidence intervals. Rows depicting different climate zones of India, while columns display long-term (1951–2020), pre-1985 (1951–1985), post-1985 (1986–2020), and most-recent (2000–2020) time periods

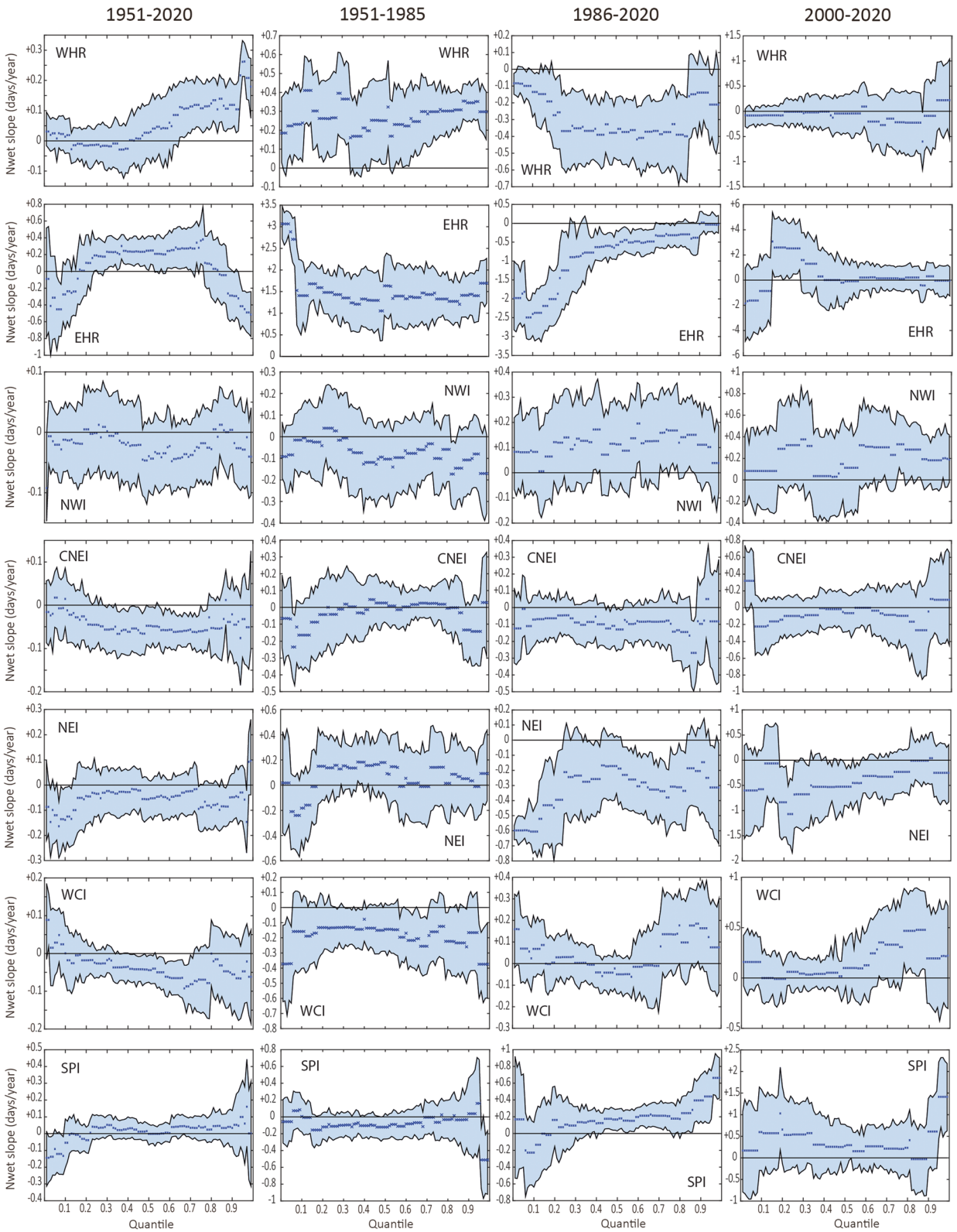

Fig. 18 Multi-temporal slope coefficient of annual rainy days (Nwet) regression line at different quantile levels (τ = 0.01–0.99). Blue points are representative of the slopes for various quantiles, black line represents zero slope i.e., no change and light blue area stands bootstrapped upper and lower 95% confidence intervals. Rows depicting different climate zones of India, while columns display long-term (1951–2020), pre-1985 (1951–1985), post-1985 (1986–2020), and most-recent (2000–2020) time periods

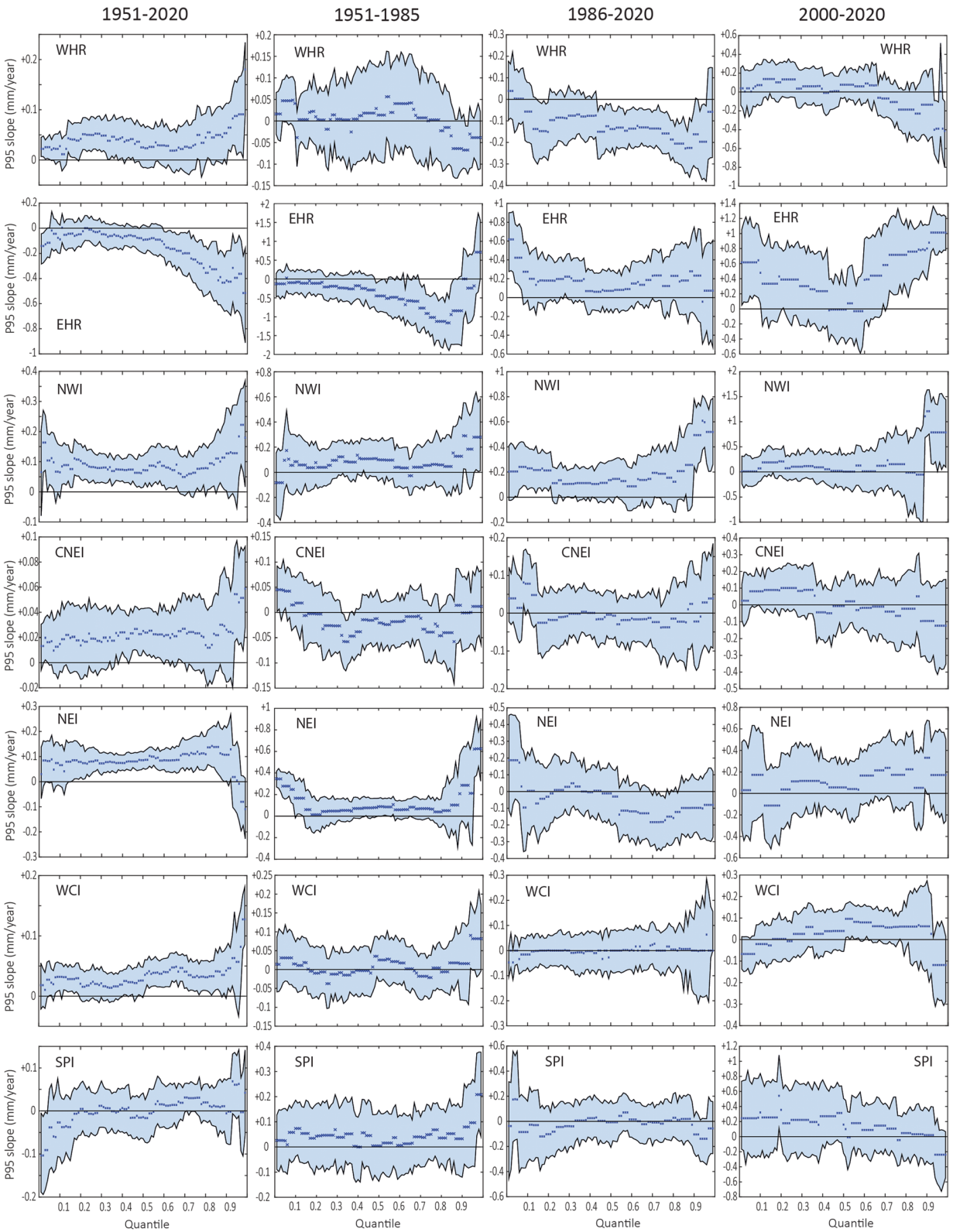

Fig. 19 Multi-temporal slope coefficient of extreme daily rainfall threshold P95 regression line at different quantile levels (τ = 0.0–0.99). Blue points are representative of the slopes for various quantiles, black line represents zero slope i.e., no change and light blue area stands bootstrapped upper and lower 95% confidence intervals. Rows depicting different climate zones of India, while columns display long-term (1951–2020), pre-1985 (1951–1985), post-1985 (1986–2020), and most-recent (2000–2020) time periods

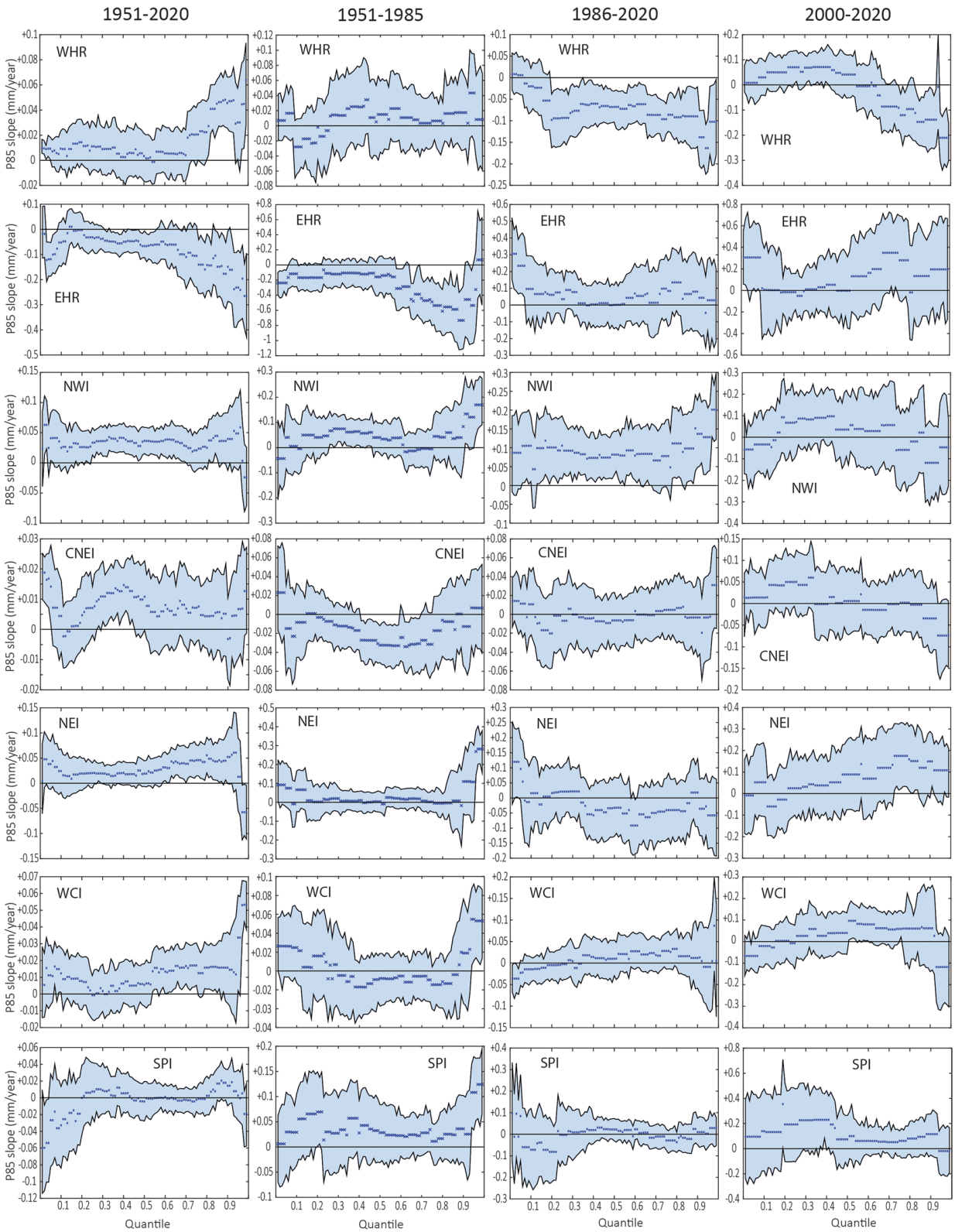

Fig. 20 Multi-temporal slope coefficient of extreme daily rainfall threshold P85 regression line at different quantile levels (τ = 0.01–0.99). Blue points are representative of the slopes for various quantiles, black line represents zero slope i.e., no change and light blue area stands bootstrapped upper and lower 95% confidence intervals. Rows depicting different climate zones of India, while columns display long-term (1951–2020), pre-1985 (1951–1985), post-1985 (1986–2020), and most-recent (2000–2020) time periods

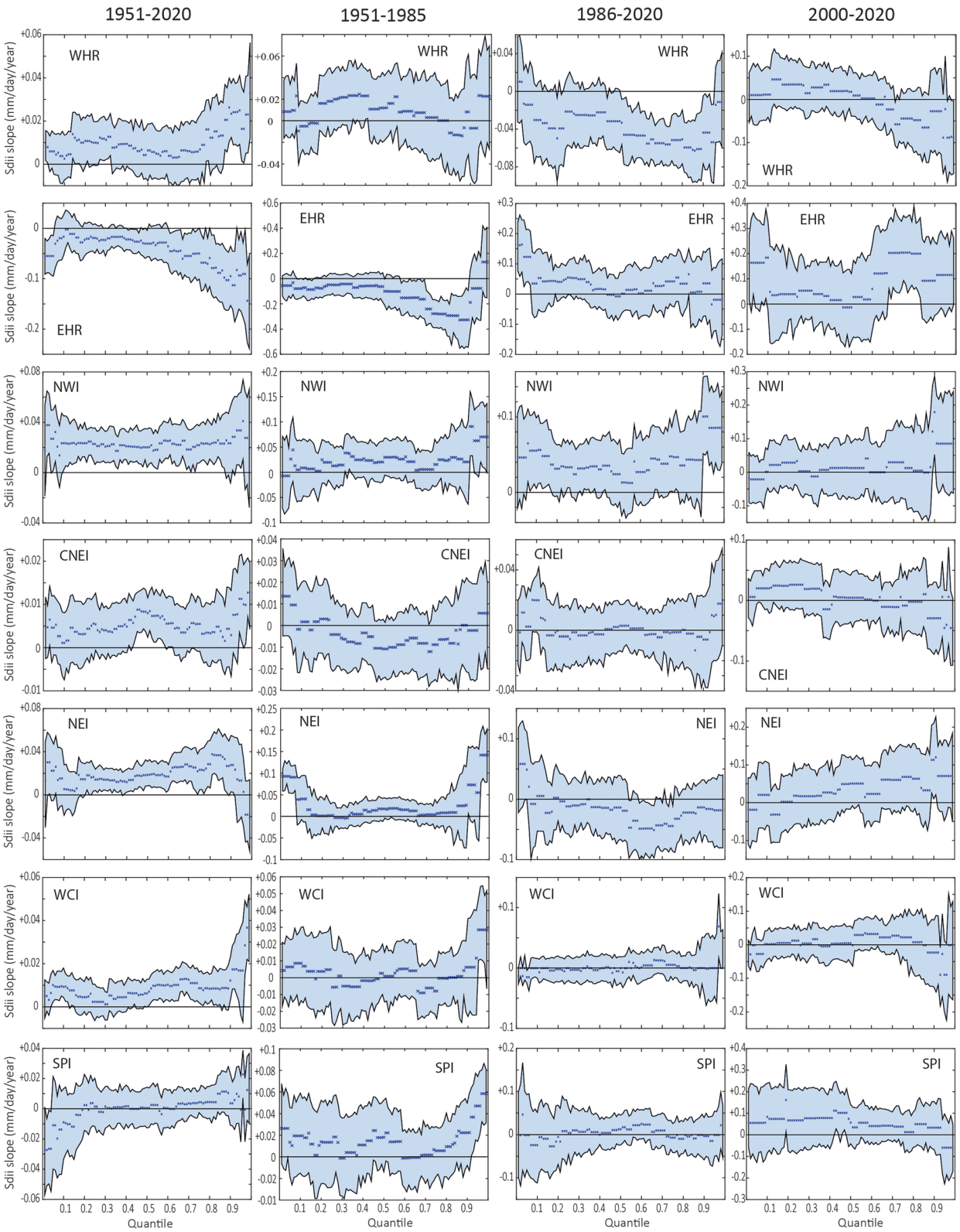

Fig. 21 Multi-temporal slope coefficient of daily rainfall intensity (Sdii) regression line at different quantile levels ($\tau = 0.01$–0.99). Blue points are representative of the slopes for various quantiles, black line represents zero slope i.e., no change and light blue area stands bootstrapped upper and lower 95% confidence intervals. Rows depicting different climate zones of India, while columns display long-term (1951–2020), pre-1985 (1951–1985), post-1985 (1986–2020), and most-recent (2000–2020) time periods

distribution of rainfall characteristics. However, the additional information about trends in QR revealed shifting of magnitude (Asum, Ssum, P95, and P85) and intensity (Sdii) rainfall characteristics towards its higher extreme tail (τ = 0.9) distribution whereas for the frequency rainfall (Nwet) characteristics, significant positive trends over India were more or less similar at lower ($\tau = 0.1$), middle ($\tau = 0.5$), and upper ($\tau = 0.9$) tail distribution. Furthermore, through an examination of the slope coefficients at various quantile (τ = 0.01–0.99) distribution associated with rainfall characteristics, its comparison at multi-temporal periods allows for the identification of trend consistency over climate zones. Most of the rainfall characteristics across WHR, EHR, and NEI showed trend instability, while comparatively NWI, CNEI, SPI, and WCI climate zones displayed less instability in trends. In summary, trend estimations of different rainfall characteristics at multi-temporal periods revealed trend inconsistencies with temporal evolution towards droughts and more intense and heterogeneously expanded extremes over Indian climate zones. These emerging patterns of rainfall characteristics over India will negatively impact rain-fed agriculture and economic development. Therefore, urgent measures are needed for enhancing water resources, agricultural management, and disaster management strategies for current and future adaptation. The results obtained from the present research may also be useful for studying net climate change over India with respect to the changing hydrometeorological regime.

Acknowledgements The Authors gratefully acknowledge the Indian Meteorological Department (IMD) for providing gridded daily rainfall data over India. The first author would like to express his appreciation to Central University of Himachal Pradesh for providing lab facilities and financial assistance in the form of Ph.D. fellowship. CK acknowledges the University Grants Commission, India, for Junior Research fellowship.

Author contribution Ashish Dogra: conceptualization, methodology, data curation, formal analysis, visualization, writing—original draft preparation, writing—reviewing and editing the manuscript; Chhabeel Kumar: data curation, visualization; Ankit Tandon: supervision, conceptualization, writing—reviewing and editing the manuscript.

Data availability The datasets generated and/or analyzed during the current study are available from the corresponding author (email: ankittandon@cuhimachal.ac.in) on reasonable request.

Declarations

Ethics approval All authors read and approved the final manuscript.

Consent to participate All authors have agreed to participate.

Consent for publication All authors have agreed to publication.

Competing interests The authors declare no competing interests.

References

Ahn K-H, Palmer R (2016) Regional flood frequency analysis using spatial proximity and basin characteristics: quantile regression vs. parameter regression technique. J Hydrol 540:515–526. https://doi.org/10.1016/j.jhydrol.2016.06.047

Allen MR, Ingram WJ (2002) Constraints on future changes in climate and the hydrologic cycle. Nature 419:224–232. https://doi.org/10.1038/nature01092

Annamalai H, Hamilton K, Sperber KR (2007) The South Asian summer monsoon and its relationship with ENSO in the IPCC AR4 simulations. J Clim 20:1071–1092. https://doi.org/10.1175/JCLI4035.1

Ashok K, Saji NH (2007) On the impacts of ENSO and Indian Ocean dipole events on sub-regional Indian summer monsoon rainfall. Nat Hazards 42:273–285. https://doi.org/10.1007/s11069-006-9091-0

Ay M (2020) Trend and homogeneity analysis in temperature and rainfall series in western Black Sea region, Turkey. Theor Appl Climatol 139:837–848. https://doi.org/10.1007/s00704-019-03066-6

Barros AP, Lettenmaier DP (1994) Dynamic modeling of orographically induced precipitation. Rev Geophys 32:265–284. https://doi.org/10.1029/94RG00625

Bhattacharyya S, Sreekesh S (2022) Assessments of multiple gridded-rainfall datasets for characterizing the precipitation concentration index and its trends in India. Int J Climatol 42:3147–3172. https://doi.org/10.1002/joc.7412

Birpınar ME, Kızılöz B, Şişman E (2023) Classic trend analysis methods' paradoxical results and innovative trend analysis methodology with percentile ranges. Theor Appl Climatol. https://doi.org/10.1007/s00704-023-04449-6

Buchinsky M (1998) Recent advances in quantile regression models: a practical guideline for empirical research. J Hum Resour 33:88–126

Cade BS, Noon BR (2003) A gentle introduction to quantile regression for ecologists. Front Ecol Environ 1:412–420. https://doi.org/10.1890/1540-9295(2003)001[0412:AGITQR]2.0.CO;2

Chatterjee S, Khan A, Akbari H, Wang Y (2016) Monotonic trends in spatio-temporal distribution and concentration of monsoon precipitation (1901–2002), West Bengal, India. Atmos Res 182:54–75. https://doi.org/10.1016/j.atmosres.2016.07.010

Choi W, Tareghian R, Choi J, Hwang CS (2014) Geographically heterogeneous temporal trends of extreme precipitation in Wisconsin, USA during 1950-2006. Int J Climatol 34:2841–2852. https://doi.org/10.1002/joc.3878

Chou C, Lan C-W (2012) Changes in the annual range of precipitation under global warming. J Clim 25:222–235. https://doi.org/10.1175/JCLI-D-11-00097.1

Darji MP, Dabhi VK, Prajapati HB (2015) Rainfall forecasting using neural network: a survey. In: 2015 International Conference on Advances in Computer Engineering and Applications. pp 706–713

Das J, Jha S, Goyal MK (2020) On the relationship of climatic and monsoon teleconnections with monthly precipitation over meteorologically homogenous regions in India: wavelet & global coherence approaches. Atmos Res 238:104889. https://doi.org/10.1016/j.atmosres.2020.104889

Dash SK, Jenamani RK, Kalsi SR, Panda SK (2007) Some evidence of climate change in twentieth-century India. Clim Change 85:299–321. https://doi.org/10.1007/s10584-007-9305-9

Dash SK, Mamgain A, Pattnayak KC, Giorgi F (2013) Spatial and temporal variations in indian summer monsoon rainfall and temperature: an analysis based on RegCM3 simulations. Pure Appl Geophys 170:655–674. https://doi.org/10.1007/s00024-012-0567-4

Datta P, Das S (2022) Assessing the consistency of trends in Indian summer monsoon rainfall. Hydrol Sci J 67:1384–1396. https://doi.org/10.1080/02626667.2022.2081507
Deshpande M, Singh VK, Ganadhi MK et al (2021) Changing status of tropical cyclones over the north Indian Ocean. Clim Dyn 57:3545–3567. https://doi.org/10.1007/s00382-021-05880-z
Dimri AP, Niyogi D, Barros AP et al (2015) Western disturbances: a review. Rev Geophys 53:225–246. https://doi.org/10.1002/2014RG000460
Dudley RW, Hirsch RM, Archfield SA et al (2020) Low streamflow trends at human-impacted and reference basins in the United States. J Hydrol 580:124254. https://doi.org/10.1016/j.jhydrol.2019.124254
Feng S, Fu Q (2013) Expansion of global drylands under a warming climate. Atmos Chem Phys 13:10081–10094. https://doi.org/10.5194/acp-13-10081-2013
Gadgil S (2003) The indian monsoon and its variability. Annu Rev Earth Planet Sci 31:429–467. https://doi.org/10.1146/annurev.earth.31.100901.141251
Gajbhiye S, Meshram C, Mirabbasi R, Sharma SK (2016) Trend analysis of rainfall time series for Sindh river basin in India. Theor Appl Climatol 125:593–608. https://doi.org/10.1007/s00704-015-1529-4
Gao M, Franzke CLE (2017) Quantile regression–based spatiotemporal analysis of extreme temperature change in China. J Clim 30:9897–9914. https://doi.org/10.1175/JCLI-D-17-0356.1
Ghosh S, Vittal H, Sharma T et al (2016) Indian summer monsoon rainfall: implications of contrasting trends in the spatial variability of means and extremes. PLoS One 11:1–14. https://doi.org/10.1371/journal.pone.0158670
Güçlü YS (2018) Multiple Şen-innovative trend analyses and partial Mann-Kendall test. J Hydrol 566:685–704. https://doi.org/10.1016/j.jhydrol.2018.09.034
Gupta V, Jain MK, Singh PK, Singh V (2020) An assessment of global satellite-based precipitation datasets in capturing precipitation extremes: a comparison with observed precipitation dataset in India. Int J Climatol 40:3667–3688. https://doi.org/10.1002/joc.6419
Haan CT (1977) Statistical methods in hydrology: Ames. IA Univ Press
Haddad K, Rahman A (2012) Regional flood frequency analysis in eastern Australia: Bayesian GLS regression-based methods within fixed region and ROI framework – quantile regression vs. parameter regression technique. J Hydrol 430–431:142–161. https://doi.org/10.1016/j.jhydrol.2012.02.012
Halpert MS, Bell GD (1997) Climate assessment for 1996. Bull Am Meteorol Soc 78:S1–S50. https://doi.org/10.1175/1520-0477-78.5s.S1
Hamed KH (2008) Trend detection in hydrologic data: The Mann–Kendall trend test under the scaling hypothesis. J Hydrol 349:350–363. https://doi.org/10.1016/j.jhydrol.2007.11.009
Hamed KH, Rao AR (1998) A modified Mann-Kendall trend test for autocorrelated data. 204:182–196
Hamilton JP, Whitelaw GS, Fenech A (2001) Mean annual temperature and total annual precipitation trends at Canadian biosphere reserves. Environ Monit Assess 67:239–275. https://doi.org/10.1023/A:1006490707949
Hassani H (2022) Singular spectrum analysis: methodology and comparison. J Data Sci 5:239–257. https://doi.org/10.6339/JDS.2007.05(2).396
Hrudya PH, Varikoden H, Vishnu R, Kuttippurath J (2020) Changes in ENSO-monsoon relations from early to recent decades during onset, peak and withdrawal phases of Indian summer monsoon. Clim Dyn 55:1457–1471. https://doi.org/10.1007/s00382-020-05335-x
Joseph PV, Gokulapalan B, Nair A, Wilson SS (2013) Variability of summer monsoon rainfall in India on inter-annual and decadal time scales. Atmos Ocean Sci Lett 6:398–403. https://doi.org/10.3878/j.issn.1674-2834.13.0044
Karandish F, Mousavi SS, Tabari H (2017) Climate change impact on precipitation and cardinal temperatures in different climatic zones in Iran: analyzing the probable effects on cereal water-use efficiency. Stoch Environ Res Risk Assess 31:2121–2146. https://doi.org/10.1007/s00477-016-1355-y
Kendall MG (1948) Rank correlation methods. Griffin, Oxford
Koenker R, Bassett G (1978) Regression quantiles. Econometrica 46:33. https://doi.org/10.2307/1913643
Konstali K, Sorteberg A (2022) Why has precipitation increased in the last 120 years in Norway? J Geophys Res Atmos 127:e2021JD036234. https://doi.org/10.1029/2021JD036234
Konwar M, Parekh A, Goswami BN (2012) Dynamics of east-west asymmetry of Indian summer monsoon rainfall trends in recent decades. Geophys Res Lett 39. https://doi.org/10.1029/2012GL052018
Koutsoyiannis D (2020) Revisiting the global hydrological cycle: is it intensifying? Hydrol Earth Syst Sci 24:3899–3932. https://doi.org/10.5194/hess-24-3899-2020
Kripalani RH, Kulkarni A, Sabade SS, Khandekar ML (2003) Indian monsoon variability in a global warming scenario. Nat Hazards 29:189–206. https://doi.org/10.1023/A:1023695326825
Laseter SH, Ford CR, Vose JM, Swift LW Jr (2012) Long-term temperature and precipitation trends at the Coweeta Hydrologic Laboratory, Otto, North Carolina, USA. Hydrol Res 43:890–901. https://doi.org/10.2166/nh.2012.067
Lausier AM, Jain S (2018) Overlooked trends in observed global annual precipitation reveal underestimated risks. Sci Rep 8:16746. https://doi.org/10.1038/s41598-018-34993-5
Malik N, Bookhagen B, Mucha PJ (2016) Spatiotemporal patterns and trends of Indian monsoonal rainfall extremes. Geophys Res Lett 43:1710–1717. https://doi.org/10.1002/2016GL067841
Mann HB (1945) Nonparametric tests against trend. Econometrica 13:245–259
Marvel K, Biasutti M, Bonfils C et al (2017) Observed and projected changes to the precipitation annual cycle. J Clim 30:4983–4995. https://doi.org/10.1175/JCLI-D-16-0572.1
Marvel K, Cook BI, Bonfils CJW et al (2019) Twentieth-century hydroclimate changes consistent with human influence. Nature 569:59–65. https://doi.org/10.1038/s41586-019-1149-8
Mondal A, Khare D, Kundu S (2015) Spatial and temporal analysis of rainfall and temperature trend of India. Theor Appl Climatol 122:143–158. https://doi.org/10.1007/s00704-014-1283-z
Mooley DA, Parthasarathy B (1984) Fluctuations in all-India summer monsoon rainfall during 1871–1978. Clim Change 6:287–301. https://doi.org/10.1007/BF00142477
O'Gorman PA, Schneider T (2009) The physical basis for increases in precipitation extremes in simulations of 21st-century climate change. Proc Natl Acad Sci 106:14773–14777. https://doi.org/10.1073/pnas.0907610106
Pachauri RK, Allen MR, Barros VR, et al (2014) Climate change 2014: synthesis report. Contribution of Working Groups I, II and III to the fifth assessment report of the Intergovernmental Panel on Climate Change. Ipcc
Pai DS, Rajeevan M, Sreejith OP et al (2014) Development of a new high spatial resolution (0.25° × 0.25°) long period (1901-2010) daily gridded rainfall data set over India and its comparison with existing data sets over the region. MAUSAM 65:1–18. https://doi.org/10.54302/mausam.v65i1.851
Pandey RP, Ramasastri KS (2001) Relationship between the common climatic parameters and average drought frequency. Hydrol Process 15:1019–1032. https://doi.org/10.1002/hyp.187
Parthasarathy B, Munot AA, Kothawale DR (1994) All-India monthly and seasonal rainfall series: 1871–1993. Theor Appl Climatol 49:217–224. https://doi.org/10.1007/BF00867461
Praveen B, Talukdar S, Shahfahad et al (2020) Analyzing trend and forecasting of rainfall changes in India using non-parametrical

and machine learning approaches. Sci Rep 10:10342. https://doi.org/10.1038/s41598-020-67228-7
Rajeevan M, Gadgil S, Bhate J (2010) Active and break spells of the Indian summer monsoon. J Earth Syst Sci 119:229–247. https://doi.org/10.1007/s12040-010-0019-4
Ramamurthy K (1969) Monsoon of India: some aspects of the "break" in the Indian southwest monsoon during July and August. Forecast Man 1:1–57
Ramesh Kumar MR, Krishnan R, Sankar S et al (2009) Increasing trend of "break-monsoon" conditions over India—role of ocean–atmosphere processes in the Indian Ocean. IEEE Geosci Remote Sens Lett 6:332–336. https://doi.org/10.1109/LGRS.2009.2013366
Rao YP (1976) Southwest monsoon, meteorological monograph. India Meteorol Dep New Delhi 366
Razavi S, Vogel R (2018) Prewhitening of hydroclimatic time series? Implications for inferred change and variability across time scales. J Hydrol 557:109–115. https://doi.org/10.1016/j.jhydrol.2017.11.053
Roxy MK, Ghosh S, Pathak A et al (2017) A threefold rise in widespread extreme rain events over central India. Nat Commun 8:708. https://doi.org/10.1038/s41467-017-00744-9
Sa'adi Z, Shahid S, Ismail T et al (2019) Trends analysis of rainfall and rainfall extremes in Sarawak, Malaysia using modified Mann–Kendall test. Meteorol Atmos Phys 131:263–277. https://doi.org/10.1007/s00703-017-0564-3
Sanikhani H, Kisi O, Mirabbasi R, Meshram SG (2018) Trend analysis of rainfall pattern over the Central India during 1901–2010. Arab J Geosci 11:437. https://doi.org/10.1007/s12517-018-3800-3
Sen PK (1968) Estimates of the regression coefficient based on Kendall's Tau. J Am Stat Assoc 63:1379–1389. https://doi.org/10.1080/01621459.1968.10480934
Şen Z (2012) Innovative trend analysis methodology. J Hydrol Eng 17:1042–1046
Şen Z (2017) Hydrological trend analysis with innovative and overwhitening procedures. Hydrol Sci J 62:294–305. https://doi.org/10.1080/02626667.2016.1222533
Sharma A, Sharma D, Panda SK (2022) Assessment of spatiotemporal trend of precipitation indices and meteorological drought characteristics in the Mahi River basin. India. J Hydrol 605:127314. https://doi.org/10.1016/j.jhydrol.2021.127314
Shepard DS (1968) A two-dimensional interpolation function for irregularly-spaced data. Proc 1968 23rd ACM Natl Conf
Shiau J-T, Huang W-H (2015) Detecting distributional changes of annual rainfall indices in Taiwan using quantile regression. J Hydro-environment Res 9:368–380. https://doi.org/10.1016/j.jher.2014.07.006
Shukla J, Wallace JM (1983) Numerical Simulation of the Atmospheric Response to Equatorial Pacific Sea Surface Temperature Anomalies. J Atmos Sci 40:1613–1630. https://doi.org/10.1175/1520-0469(1983)040<1613:NSOTAR>2.0.CO;2
Singh D, Ghosh S, Roxy MK, McDermid S (2019) Indian summer monsoon: extreme events, historical changes, and role of anthropogenic forcings. WIREs Clim Chang 10:e571. https://doi.org/10.1002/wcc.571
Singh A, Thakur S, Adhikary NC (2021) Analysis of spatial and temporal rainfall characteristics of the North East region of India. Arab J Geosci 14:885. https://doi.org/10.1007/s12517-021-07266-1
Sonali P, Nagesh Kumar D (2013) Review of trend detection methods and their application to detect temperature changes in India. J Hydrol 476:212–227. https://doi.org/10.1016/j.jhydrol.2012.10.034
Srivastava PK, Han D, Rico-Ramirez MA, Islam T (2014) Sensitivity and uncertainty analysis of mesoscale model downscaled hydro-meteorological variables for discharge prediction. Hydrol Process 28:4419–4432. https://doi.org/10.1002/hyp.9946
Suthinkumar PS, Varikoden H, Babu CA (2023) Changes in extreme rainfall events in the recent decades and their linkage with atmospheric moisture transport. Glob Planet Change 221:104047. https://doi.org/10.1016/j.gloplacha.2023.104047
Tareghian R, Rasmussen P (2013) Analysis of Arctic and Antarctic sea ice extent using quantile regression. Int J Climatol 33:1079–1086. https://doi.org/10.1002/joc.3491
Theil H (1950) A rank-invariant method of linear and polynomial regression analysis, Part I. Proc. R. Netherlands Acad Sci
Treppiedi D, Cipolla G, Francipane A, Noto LV (2021) Detecting precipitation trend using a multiscale approach based on quantile regression over a Mediterranean area. Int J Climatol 41:5938–5955. https://doi.org/10.1002/joc.7161
Uranchimeg S, Kwon H-H, Kim B, Kim T-W (2020) Changes in extreme rainfall and its implications for design rainfall using a Bayesian quantile regression approach. Hydrol Res 51:699–719. https://doi.org/10.2166/nh.2020.003
Varikoden H, Babu CA (2015) Indian summer monsoon rainfall and its relation with SST in the equatorial Atlantic and Pacific Oceans. Int J Climatol 35:1192–1200. https://doi.org/10.1002/joc.4056
Varikoden H, Revadekar JV, Kuttippurath J, Babu CA (2019) Contrasting trends in southwest monsoon rainfall over the Western Ghats region of India. Clim Dyn 52:4557–4566. https://doi.org/10.1007/s00382-018-4397-7
Vidya PJ, Ravichandran M, Subeesh MP, Sourav C, Nuncio M (2020) Global warming hiatus contributed weakening of the Mascarene High in the Southern Indian Ocean Abstract Scientific Reports 10(1). https://doi.org/10.1038/s41598-020-59964-7
Westra S, Alexander LV, Zwiers FW (2013) Global increasing trends in annual maximum daily precipitation. J Clim 26:3904–3918. https://doi.org/10.1175/JCLI-D-12-00502.1
Wilhite DA, Glantz MH (1985) Understanding: the drought phenomenon: the role of definitions. Water Int 10:111–120. https://doi.org/10.1080/02508068508686328
Xavier A, Kottayil A, Mohanakumar K, Xavier PK (2018) The role of monsoon low-level jet in modulating heavy rainfall events. Int J Climatol 38:e569–e576 https://doi.org/10.1002/joc.5390
Xu ZX, Takeuchi K, Ishidaira H (2003) Monotonic trend and step changes in Japanese precipitation. J Hydrol 279:144–150. https://doi.org/10.1016/S0022-1694(03)00178-1
Yue S, Wang C (2004) The Mann-Kendall test modified by effective sample size to detect trend in serially correlated hydrological series. Water Resour Manag 18:201–218. https://doi.org/10.1023/B:WARM.0000043140.61082.60